Molecular Vision 2026; 32:210-230 <http://www.molvis.org/molvis/v32/210>
Received 4 April 2025 | Accepted 10 June 2026 | Published 12 June 2026

Toll-like receptor 9 in retinal pigment epithelial cells: Expression, function and the role of TGF-β1

Elisabeth Esser,[1] Heidrun Kuhrt,[2] Focke Ziemssen,[1] Margrit Hollborn[1]

[1]Department of Ophthalmology and Eye Hospital, University of Leipzig, Leipzig, Germany; [2]Institute of Anatomy, University of Leipzig, Germany

Purpose: Inflammatory processes in the aged retina may be exacerbated by systemic infection with viruses and bacteria, potentially aggravating age-related macular degeneration (AMD). Toll-like receptors (TLR) are key mediators in detecting pathogen-associated molecular patterns (PAMPs) and host-derived damage-associated molecular patterns (DAMPs). This study aimed to investigate *TLR* gene expression in cultured retinal pigment epithelial (RPE) cells, focusing particularly on TLR9.

Methods: TLR gene expression was assessed using semiquantitative qPCR, while protein expression was evaluated through western blotting, immunocytochemistry, and ELISA. Hypoxic conditions were simulated using $CoCl_2$ or by incubation in a 0.1% O_2 atmosphere. RPE cell proliferation and viability were examined using bromodeoxyuridine (BrdU) and MTT assays. Cell necrosis and apoptosis were analyzed with a cellular DNA fragmentation ELISA.

Results: Among the *TLRs* analyzed, *TLR9* showed the most pronounced upregulation under hypoxic conditions. TLR9 protein expression was similarly induced by $CoCl_2$ as well as in a 0.1% O_2 atmosphere. Hypoxia increased the protein levels of γH2A.X, a marker for DNA damage and cellular senescence. The TLR9 agonist ODN 1826 induced the gene expression of downstream signaling molecules (*MYD88*, *IRF7, RELA*), inflammatory factors (*IFNA, COX2*), and *MMP9* as well as the secretion of TGF-β1. These effects were reversed by TLR9 inhibitors (ODN 2088 and ODN INH-18). Transforming growth factor (TGF)-β1 significantly suppressed the TLR9 expression at both the mRNA and protein levels. This suppressive effect was reversed at the RNA level by inhibiting components of the TGF-β1 signaling pathway, including activin receptor-like kinase (ALK), Smad3, p38 mitogen-activated protein kinase (p38 MAPK), c-Jun N-terminal kinase (JNK), and phosphatidylinositol 3-kinase (PI3K) under hypoxic conditions.

Conclusions: TLR9 activation under hypoxic conditions initiates pro-inflammatory pathways in RPE cells. In the aging retina, viral and bacterial infections and/or DAMPs may further amplify these responses, worsening retinal degeneration. TGF-β1 may exert protective, anti-inflammatory effects by downregulating TLR9 expression.

Age-related macular degeneration (AMD) is associated with chronic inflammation [1-3] and immunological abnormalities like local activation of the alternative complement cascade [4,5]. Drusen contain various components of complement and other proteins involved in immune-mediated inflammatory processes [6,7]. Retinal inflammation is associated with systemic inflammation and macrophage activation and may be triggered by multiple factors, including genetic and systemic health factors [8]. Inflammatory processes in the aged retina are likely to be exacerbated by chronic systemic infections with viruses and bacteria [9-12]. Injection of viral double-stranded RNA (dsRNA), a component of drusen [13], into the subretinal space of mice was shown to induce necrosis of the retinal pigment epithelium (RPE) and macrophage infiltration into the outer retina [14].

Correspondence to: Margrit Hollborn, Department of Ophthalmology and Eye Hospital, University of Leipzig, Faculty of Medicine, Liebigstrasse 10-14, D-04103 Leipzig, Germany Phone: +49 (0) 341 97 21 561; FAX: +49(0) 341 97 21 659; email: hollbm@medizin.uni-leipzig.de

The RPE plays a crucial role as a first-line defense in the retina by protecting against invading pathogens like viruses and bacteria, and initiating innate immune responses. Key mediators in microbial recognition are Toll-like receptors (TLRs) [15]. To date, ten functional TLRs were identified in humans. These receptors are located at the cell surface (TLRs 1, 2, 4, 5, 6) or within intracellular membranous organelles like endosomes, lysosomes, and endoplasmic reticulum (TLRs 3, 7, 8, 9) [16]. TLRs recognize conserved pathogen-associated molecular patterns (PAMPs) produced by viral, bacterial, and fungal pathogens [17]. Upon ligand binding, TLR signaling induces inflammatory responses by promoting the production of cytokines, chemokines, and adhesion molecules. Cell surface TLRs primarily recognize microbial membrane components such as lipids or lipoproteins, while intracellular TLRs detect viral or bacterial nucleic acids.

In addition to PAMPs, TLRs also recognize endogenous molecules known as damage-associated molecular patterns (DAMPs), host-derived signals released during cellular stress or damage, which contribute to sterile inflammation. For example, TLR9, located in the endoplasmic reticulum

of various immune cells, detects DNA fragments with unmethylated CpG-DNA motifs. These can originate from proliferating or dying microbes and mitochondria of damaged host cells [18-20]. Downstream TLR signaling requires the recruitment of adaptor molecules and leads to activation of nuclear factor (NF)-κB and interferon (IFN) regulatory factor (IRF) pathways. Specifically, TLR9 activation induces type I interferon via the myeloid differentiation primary response 88 (MYD88)-IRF7 pathway and inflammatory cytokines via the MYD88-NF-κB pathway [16,21-23].

It has been shown that RPE cells express several TLR subtypes, including TLRs 2, 3, and 9 [24-28]. Activation of TLRs stimulates the production of inflammatory cytokines and angiogenic factors such as interleukins (IL)-1β, IL-6, tumor necrosis factor α (TNFα), monocyte chemoattractant protein 1 (MCP-1), vascular endothelial growth factor (VEGF), and basic fibroblast growth factor (bFGF) in RPE cells [25-27].

Transforming growth factor-beta (TGF-β1, TGF-β2 and TGF-β3) are multifunctional cytokines of the TGF-β family, and all have been identified in the human eye [29,30]. They are secreted in a latent inactive form and can be converted into their biologically active form by the activity of matrix metalloproteinase (MMP) [31]. TGF-β signals through a transmembrane receptor complex composed of TGF-β receptor type I (ALK5) and type II receptors, activating either canonical (SMAD-dependent) or non-canonical (e.g., mitogen-activated protein kinase MAPK; c-Jun-N-terminal kinase JNK; phosphatidylinositol 3-kinase PI3K) pathways [32]. The role of TGF-β in neovascular AMD (nAMD) is controversial [33]. On one hand, TGF-β acts as a pro-angiogenic factor by increasing the expression of VEGF-A in RPE cells [34] or through VEGF-A-independent signaling [35]. On the other hand, it protects retinal vessels [36]. TGF-β is also known to be a negative regulator of TLR signaling by suppression of adaptor protein MyD88, which could be a reason for its anti-inflammatory effect [37].

Although viral and/or bacterial infections are considered risk factors for AMD [9-11], there is limited knowledge about the regulation of TLR expression and especially TLR9 function under pathological conditions in RPE cells. The focus was on TLR9, a sensor for unmethylated CpG DNA, which can originate by damaged host cells, among other sources. Another reason is its role in the development of lifestyle-related diseases [38]. To investigate this, the primary aim of the present study was to compare *TLR* gene expressions in acutely isolated versus cultured human RPE cells and to evaluate changes under pathological conditions. Specifically, we investigated the effects of hypoxia and extracellular hyperosmolarity. Retinal hypoxia is a major pathogenic feature in AMD [39]. Since hypertension is a risk factor of AMD and diabetic retinopathy [40,41], and because high extracellular NaCl directly affect RPE cells by stimulating inflammatory and angiogenic responses [42,43] we also tested high NaCl-induced hyperosmolarity. The second objective was to determine whether activation and blockade of TLR9 alters the expression of inflammatory and angiogenic genes in cultured RPE cells under these conditions. Finally, we analyzed the role of TGF-β1 in regulating TLR9 expression.

METHODS

Ethics statement: The study followed the tenets of the Declaration of Helsinki for the use of human subjects. The use of human material was approved by the Ethics Committee of the University of Leipzig (#745, 07/25/2011). Post-mortem eyes from human cornea donors without reported eye disease were obtained within 48 h after death with the written informed consent from the relatives to the use of retinal tissue in basic science.

Materials: Cell culture components and solutions were purchased from Gibco BRL (Paisley, UK), and fetal bovine serum was from Invitrogen (Paisley, UK). Human recombinant proteins such as transforming growth factor-β1 (TGF-β1), and VEGF-A_{165} were from R&D Systems (Abingdon, UK). The inhibitory oligodeoxynucleotide (iODN) iODN 2088, iODN INH-18, the control ODN co-ODN 2088, and the TLR9 agonist ODN 1826 were purchased from InvivoGen (San Diego, CA). The following selective pharmacological inhibitors were obtained from Tocris (Ellisville, MO): 666–15, LY294002, PD98059, SB203580, SP600125. SB431542, and SIS3 were purchased from Sigma (Deisenhofen, Germany). Anti TGF-β Pan Specific neutralizing antibody was from R&D Systems (Abingdon, UK). All other antibodies used for western blotting or immunocytochemical staining. Actinomycin D, and human recombinant α-thrombin, and all other used agents were sourced from Sigma-Aldrich (Taufkirchen, Germany), unless specified otherwise.

Cell culture: RPE cells were prepared and cultured as described previously [43]. Cultured cells of passages 3 - 5 were used. Cells which achieved a confluence of approximately 90% were cultured for 16 h in serum-free medium. During this period, 100% confluence was achieved. Thereafter, test substances were given to the serum-free medium. Hyperosmotic media was made by adding NaCl (+100 mM) or sucrose (+200 mM). Extracellular hypoosmolarity (60% osmolarity) was established by adding distilled water. Hypoxia and chemical hypoxia were established by cell culture in a 0.1% O_2-atmosphere or by addition of 150 µM

of the hypoxia mimetic $CoCl_2$, respectively. $CoCl_2$ mimics hypoxic conditions by stabilization of hypoxia-inducible transcription factor (HIF)-1α and HIF-2α under normoxic conditions [44]. Inhibitory agents were added 30 min before the start of the tests.

RNA extraction and cDNA synthesis: Total RNA was extracted using the InviTrap Spin Universal RNA Mini Kit (Stratec Molecular, Berlin, Germany). The A_{260}/A_{280} ratio of the optical density of RNA samples was measured using NanoDrop1000 (peQLab, Erlangen, Germany) and was between 1.95 and 2.05 which indicates adequate RNA quality. After the use of DNase I (Roche, Mannheim, Germany), cDNA was synthesized from 0.25 µg RNA using a reverse transcription kit (ThermoFisher Scientific, Waltham, MA).

Quantitative real-time-PCR analysis (qPCR): QPCR was performed using the CFX Connect Real-Time PCR System (BioRad, Munich, Germany) with primer pairs described in (Appendix 1). The amplification mixture (10 µl) contained 5 µl of 2x SsoAdvanced™ Universal SYBR Green Supermix (BioRad), specific primer set (0.2 µM each), 1 µl (25 ng) of cDNA. The amplification conditions were: enzyme activation and cDNA denaturation at 95 °C for 30 s (one cycle), 45 cycles denaturation (95 °C, 15 s), annealing and extension (60 °C; 45 s), and melting curve (the temperature was increased from 65 °C to 95 °C in 0.5 °C steps). The correct length of PCR products was verified using agarose gel electrophoresis and checked by the specific melting temperature. The level of ACTB and B2M mRNA were used to normalize mRNA expression in cells cultured under hypoxic conditions ($CoCl_2$, 0.1% O_2). The stability of these housekeeping genes and their use for normalizing the results were checked according to Pfaffl et al. [45]. A calculated standard deviation (SD) <1 indicates sufficient stability of the housekeeping gene. All other mRNA levels were normalized to the level of *ACTB* mRNA. Relative mRNA expression levels were calculated according to the $2^{-\Delta\Delta CT}$ method [46].

Immunocytochemistry: RPE cell cultures were fixed with 4% paraformaldehyde for 15 min on ice and washed with prechilled phosphate-buffered saline (PBS; pH 7.4; Invitrogen). PBS plus 0.3% Triton X-100 was added for 15 min at room temperature (RT). Blocking of nonspecific antibody binding was performed using PBS containing 10% normal goat serum and 0.3% Triton X-100 for 2 h at RT. Subsequently the cells were incubated with primary antibodies diluted in blocking solution at 4 °C overnight. After washing with PBS plus 0.3% Triton X-100, cells were incubated with the secondary antibodies for 1 h at RT. After further washing steps, cell nuclei were stained with 4',6-diamidin-2-phenylindol (DAPI; 1:10.000; Invitrogen) for 15 min at RT. The coverslips were mounted using Fluorescence Mounting Medium (DakoCytomation, Glostrup, Denmark). Images were taken using the fluorescence microscope Olympus BX40 (Olympus, Essex, UK) with a CCD camera (Olympus XM10) and the cellSens software (Olympus). The used antibodies are listed in Appendix 2.

Western blot analysis: Protein extracts from acutely isolated neuroretinas of two individual donors were prepared using the Mammalian Cell lysis kit (MCL-1; Sigma-Aldrich) according to the manufacturer's instructions. For preparing cytosolic (soluble proteins) and membrane protein extracts RPE cells were cultured in 75-cm^2 culture flasks in F-10 medium containing 10% FBS until confluence was reached. Then the medium was removed, the cells were washed with prechilled PBS and detached from the culture flasks using a cell scraper. After centrifugation, the cells were lysed in 0.5 ml buffer A (50 mM Tris-HCl (pH 7.4), 150 mM NaCl, 1 mM EDTA, 1% protease inhibitor cocktail, and 1% phosphatase inhibitor cocktail (both from Sigma-Aldrich), and 0.5% PMSF (phenylmethylsulfonyl fluoride). The lysates were centrifuged at 20,817 ×g for 15 min at 4 °C and the supernatants (soluble cytosolic proteins) were removed. The remaining pellets were solubilized in 400 µl of buffer B that (50 mM Tris-HCl (pH 7.4), 150 mM NaCl, 1 mM EDTA, 1% Triton X-100, 0.1% SDS, 1% protease inhibitor cocktail, and 1% phosphatase inhibitor cocktail).

For preparing whole cell protein extracts the following lysis buffer (180 µl; 50 mM Tris-HCl (pH 8.0), 5 mM EDTA, 150 mM NaCl, 0.5% phenylmethylsulfonyl fluoride, 0.5% NP-40 detergent solution (Thermo Fisher Scientific), 1% protease inhibitor cocktail, and 1% phosphatase inhibitor cocktail (Sigma-Aldrich)) was used. Equal amounts of protein (30 µg and 35 µg, respectively) were separated by 12.5% or 10% SDS–PAGE. The protein amounts and the quality of the protein transfer to the PVDF membranes were routinely checked using Ponceau S staining. Primary and secondary antibodies (Appendix 2) were applied. For visualization of the immunoreactive bands 5-bromo-4-chloro-3-indolyl phosphate/nitro blue tetrazolium were used. The ChemiDoc™ Imaging System (BioRad) was used for taking images and preparing densitometric evalution.

ELISA, DNA fragmentation, cell proliferation and viability assays: RPE cells were cultured and stimulated in 12-well plates. Thereafter, cell culture supernatants were collected and the amount of secreted VEGF-A (DVE00; R&D Systems) and TGF-β1 (DB100C; R&D Systems) were determined by ELISA using 200 µl and 100 µl supernatant, respectively.

To analyze cell necrosis or apoptosis the Cellular DNA Fragmentation ELISA (Roche) was used. 5×10^3 cells were

seeded per well in 96-well plates and cultured until approximately 90% confluence was reached. Afterwards the cells were pre-labeled with bromodeoxyuridine (BrdU) for 16 h and then the cells were cultured in presence or absence of $CoCl_2$, NaCl or in a 0.1% O_2 atmosphere for further 24 h. Detected BrdU-labeled DNA fragments in cell free supernatants indicate necrosis and in cell lysates indicate apoptosis.

To determine cell viability and proliferation rate, cells were cultured for 24 h in the presence of high NaCl (+100 mM), $CoCl_2$ (150 µM) or in a 0.1% O_2 atmosphere, respectively, and in the absence or presence of iODN INH-18 (2.5 µM), iODN 2088 (1 µM). Incorporation of BrdU was measured using the Cell Proliferation ELISA BrdU Kit (Roche). BrdU (10 µM) was applied 5 h before fixation of the cultures. The absorbance was determined at 450 nm using Spectra Max 50 (Molecular Devices, Sunnyvale, CA). Cell viability was evaluated using a 3-(4,5-dimethylthiazol-2-yl)-2,5-diphenyltetrazolium bromide (MTT) assay (Serva, Heidelberg, Germany). MTT solution (10 µl; 5 mg/ml) was given to each well 4 h before cessation of the cell culture. Culture supernatants were removed and DMSO (100 µl) was added. The absorbance was measured at 570 nm.

Quantification of cell-free DNA: The amount of cell-free DNA in culture supernatants was determined using the NanoDrop1000 (peQLab). Therefore, 1 µl of cell culture supernatant (untreated control, NaCl, $CoCl_2$, 0.1% O_2) was used for the measurement. Each measurement was performed in triplicate. F-10 medium without FBS, which was used for the cell culture experiments, served as a blank.

Statistical analysis: At least three independent experiments with cells of different donors were performed for each test. Data are presented as means ± SEM. Statistical analysis was performed with Graphpad Prism Version 6.07 (Graphpad Software, San Diego, CA). Cell viability, cytokine and cell free DNA content of the supernatants, DNA fragmentation, and western blot signals are expressed as percent of untreated control (100%). PCR results are shown as x-fold change to untreated control (1).

The nonparametric Mann–Whitney U test for single comparisons two groups without normal distribution of data was used to analyze the qPCR, cell viability and DNA fragmentation results. The one-sample *t* test was used to compare the qPCR results from the experiments with pharmacological inhibitors. This test takes into account the variability of the values obtained from the signals of the control cells, even though these occur without standard deviations (SD=0). One-way ANOVA (ANOVA) followed by Bonferroni's multiple comparison test was used to compare western blot and ELISA results of multiple groups from differently treated cells. Differences with $p<0.05$ were considered as significant.

RESULTS

TLR gene expression in human RPE cells: QPCR analysis was performed to examine the expression of *TLR* genes in RPE cells. The analysis was done with cells which were acutely isolated from eyes of post-mortem human donors (differentiated cells) and with cultured cells (dedifferentiated cells). Transcripts of all 10 human *TLR* genes were detected in the total RNA extracted from acutely isolated RPE cells (Figure 1A). Cultured RPE cells also expressed multiple *TLR* genes; the levels of *TLR7*, *TLR8*, and *TLR10* gene transcripts were below the detection threshold (Figure 1B). The levels of *TLR1*, *TLR2*, *TLR5*, and *TLR9* transcripts were smaller in cultured than in acutely isolated cells, as indicated by the significantly ($p<0.05$) higher number of cycles required to detect the transcripts in cultured cells (Figure 1B). The cycle numbers necessary to detect *TLR3*, *TLR4* and *TLR6* transcripts were not significantly ($p>0.05$) different between acutely isolated and cultured cells (Figure 1B).

Regulation of TLR gene expression: We tested different agents to screen which pathogenic conditions alter the expression levels of *TLR* genes in cultured RPE cells. The hypoxia mimetic $CoCl_2$ [44] induced a significant ($p<0.05$) increase of the cellular level of *TLR4* and *TLR9* transcripts after 24 h of stimulation and slightly reduced mRNA levels of *TLR3* (Figure 2A). The stimulatory effect of $CoCl_2$-induced hypoxia on the *TLR9* gene expression as well as the reduction of *TLR3* mRNA amount were confirmed in cells cultured in a 0.1% O_2-atmosphere. Compared to $CoCl_2$, the extent of *TLR9* induction was lower and a slight significant increase was already observed after 2 h of stimulation. In contrast to the $CoCl_2$ results an induction of TLR2 mRNA was found under these conditions and the increase of TLR4 expression was no longer detectable (Figure 2B). Oxidative stress induced by addition of H_2O_2 (20 µM) to the culture medium did not alter the expression of the *TLR* genes investigated (not shown). Extracellular hyperosmolarity produced by addition of 100 mM NaCl to the culture medium induced increases of the *TLRs 1*, *4*, *6*, and *9* gene expression and did not alter the expression of *TLRs 2*, *3*, and *5* genes (Figure 2C). Addition of 200 mM sucrose, which caused an increase in osmolarity equal to 100 mM NaCl, induced a similar elevation of the *TLR9* mRNA level as addition of NaCl (Figure 2D). This suggests that high NaCl induces *TLR9* gene expression by elevation of the extracellular osmolarity and not by the change of the NaCl gradient across the plasma membrane. The $CoCl_2$- and high NaCl-induced *TLR9* gene expression

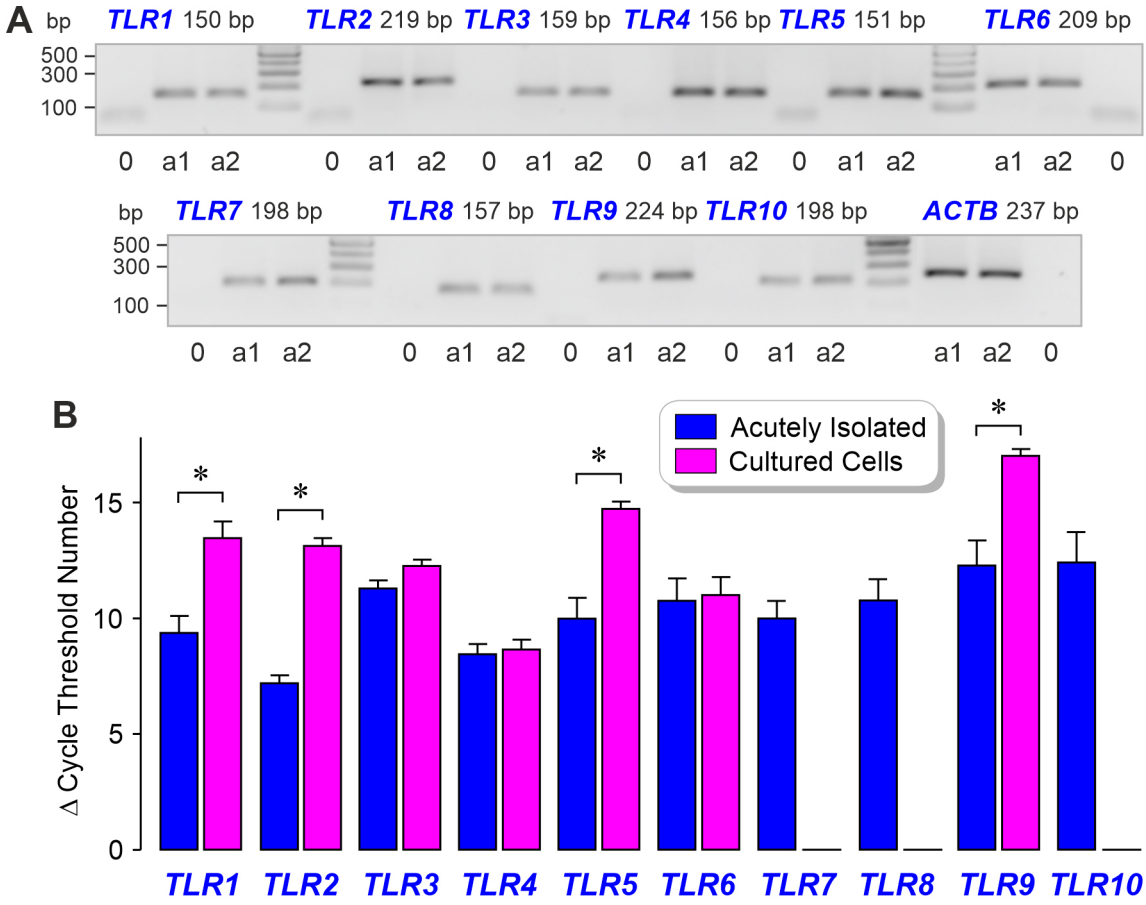

Figure 1. Expression of Toll-like receptor (*TLR*) genes in human RPE cells. **A**: Agarose gel electrophoresis images of gene transcripts which was performed with PCR products of acutely isolated cells from two different post-mortem donors (a1, a2). 0, negative control done by adding double-distilled water instead of cDNA as a template. β-actin (*ACTB*) mRNA was used to normalize *TLR* mRNA levels in qPCR analysis. **B**: Comparison of *TLR* gene expression levels in acutely isolated and cultured RPE cells. The data were determined by qPCR. The bars show the mean of cycle numbers at the threshold of transcript detection ± SD. Cells derived from 5 (acutely isolated) and 9 (cultured) donors, respectively, were used. The statistical analysis was performed using non-parametric Mann–Whitney-U-Test. Significant difference between acutely isolated and cultured cells: *p<0.05.

was fully prevented by actinomycin D (5 µg/ml; Appendix 3) which blocks RNA polymerase II, suggesting that the expression was mediated by induction of gene transcription; the *TLR9* mRNA stability was not different to cells cultured under control conditions (Appendix 3). VEGF, a growth factor associated with pathological angiogenesis was without effect whereas the multifunctional TGF-β1 reduced the *TLR9* mRNA in a time dependent manner (Figure 2G). We also found that FBS (10%, serum) and thrombin caused downregulation of the *TLR9* gene expression (Figure 2F). Triamcinolone acetonide, an anti-inflammatory corticosteroid clinically used together with anti-VEGF drugs to achieve a greater effect than monotherapy in different retinopathies [47] increased *TLR9* mRNA in RPE cells after 24 h of stimulation (Figure 2H).

TLR9 protein in cultured RPE cells: Cultured RPE cells showed a strong intracellular and a weak TLR9 immunoreactivity in cell membranes (Figure 3A). Western blot analysis of cytosolic (soluble proteins) and membrane protein extracts of cultured RPE cells displayed a TLR9-immunoreactive band around 113 kDa (Figure 3B). Blots of membrane protein extracts showed a more intensely stained immunoreactive band compared to blots of cytosolic proteins (Figure 3B). As a positive control, the presence of immunoreactive TLR9 in lysates of acutely isolated neuroretinas from two donors was verified (Figure 3B). The data indicate that TLR9 protein is predominantly localized to RPE cell membranes. High extracellular osmolarity (NaCl), hypoxia induced by $CoCl_2$ or by cultivation of RPE cells in a 0.1% O_2 atmosphere, and triamcinolone strongly induced (Figure 2A-C,H) whereas TGF-β1

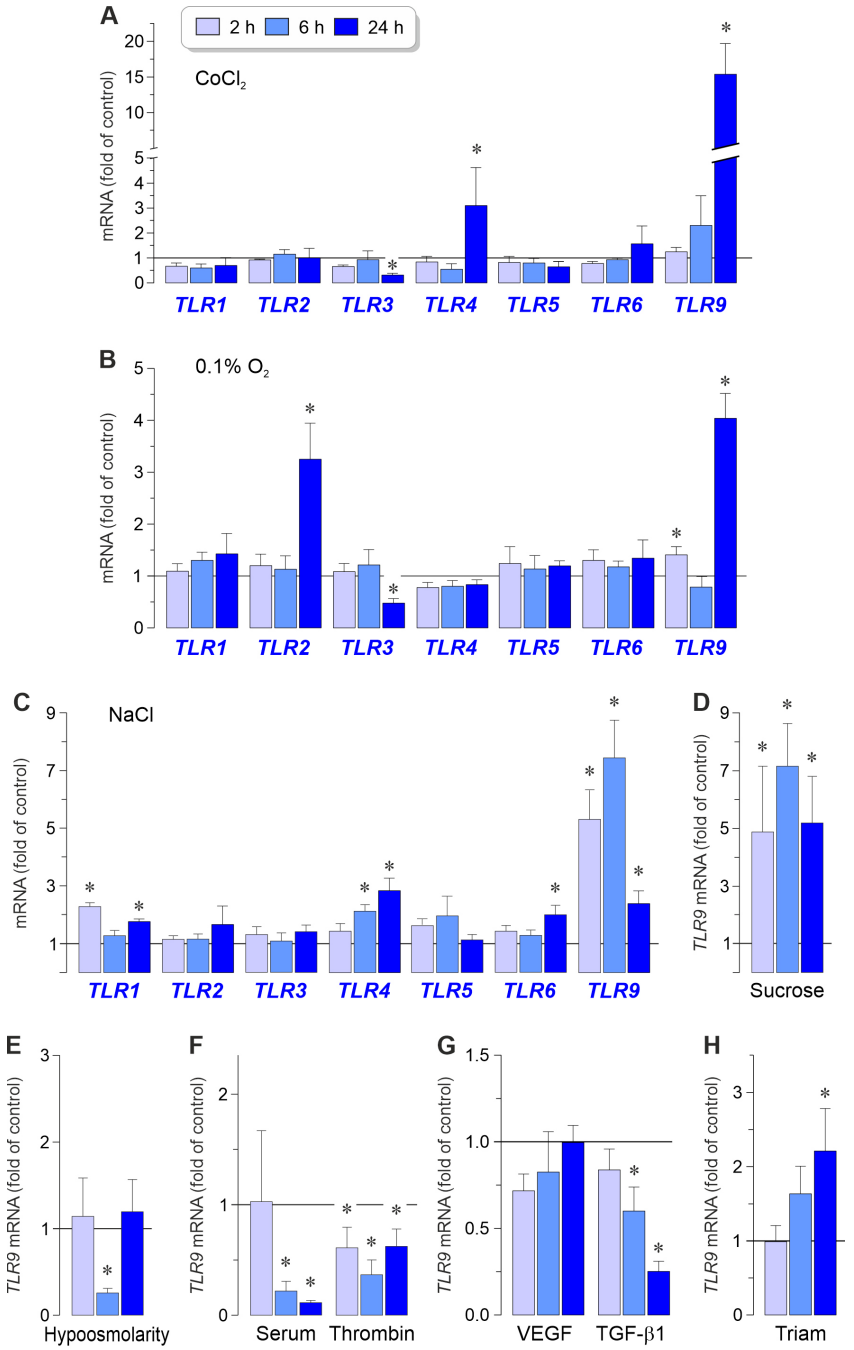

Figure 2. Regulation of *TLR* gene expression in cultured human RPE cells. Relative mRNA levels were evaluated by qPCR and are shown as folds of unstimulated control. The cells were stimulated for 2, 6, and 24 h, as indicated by the color of the bars. **A**: Effect of chemical hypoxia induced by $CoCl_2$ (150 µM, n=3–5). **B**: Effect of cell culture in a 0.1% O_2 atmosphere on the *TLR* gene expression (n=4). **C**: Effect of extracellular hyperosmolarity induced by addition of 100 mM NaCl to the culture medium (n=3–5). **D:** Effect of addition of 200 mM sucrose (n=3–4) and (**E**) extracellular hypoosmolarity (60% osmolarity, n=5) on the *TLR9* gene expression. **F**: Effects of fetal bovine serum (10%, n=3–4) and thrombin (10 U/ml, n=4–5) on the *TLR9* gene expression (**G**). Influence of growths factors such as VEGF (n=5) or TGF-β1 (n=3; each 10 ng/ml) on *TLR9* gene expression. **H**: Effect of Triamcinolone acetonide (50 µM) on *TLR9* mRNA (n=4–5). *ACTB* and *B2M* were used to normalize the results for $CoCl_2$ as well as 0.1% O_2. *ACTB* was used to normalize the results of NaCl, sucrose, hypoosmolarity, serum, thrombin, VEGF, TGF-β1, and Triamcinolone. Each bar represents data from independent experiments using cells from different donors. The statistical analysis was performed using the non-parametric Mann–Whitney-U-Test. Results are shown as mean ± SEM. Significant difference versus unstimulated control: *p<0.05.

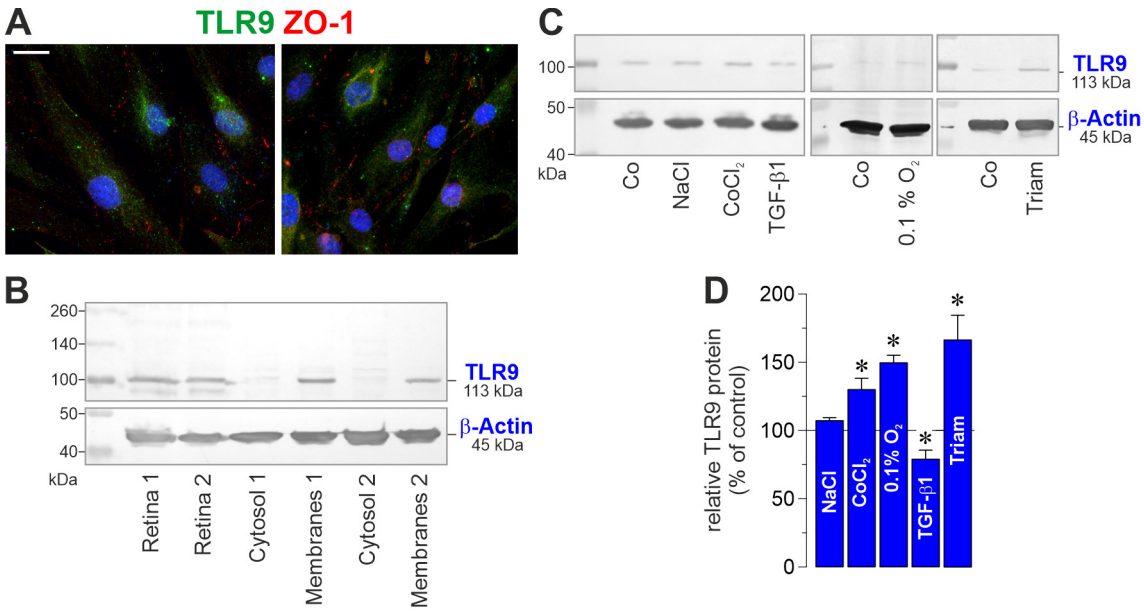

Figure 3. TLR9 protein in cultured human RPE cells. **A**: Immunolabeling of cultured RPE cells with an anti-TLR9 antibody (*green*) and an antibody against the tight junction protein zonula occludens-1 (ZO-1; *red*). Cell nuclei are labeled with DAPI (*blue*). Bars, 20 µm. **B**: western blots of TLR9 protein performed with lysates of acutely isolated neuroretinas and cytosolic and membrane protein extracts of cultured RPE cells derived from two donors (1, 2). **C**: Representative western blots of TLR9 protein with lysates of RPE cells incubated in presence of NaCl (+100 mM), hypoxia mimetic $CoCl_2$ (150 µM), TGF-β1 (10 ng/ml), in a 0.1% O_2 atmosphere or Triamcinolone acetonide (Triam; 50 µM) for 24 h. β-actin served as loading control. **D**: Densitometric evaluation of the western blot results. β-actin was used to normalize the results. The data were obtained from 3 (TGF-β1) and 4 (NaCl, $CoCl_2$, 0.1% O_2, Triam) independent experiments using RPE cells from different donors. Significant difference versus unstimulated control: *p<0.05. The statistical analysis was performed using the One-way ANOVA followed by Bonferroni's multiple comparison test.

significantly reduced the *TLR9* mRNA amount (Figure 2G). Except NaCl, these results were confirmed at the protein level (Figure 3C,D).

γH2A.X as sign for DNA damage and cellular senescence: TLR9 is known as a sensor for endogenous DNA fragments [20,23]. Because *TLR9* mRNA was induced by hypoxia and high extracellular osmolarity we wanted to know if these conditions alter the expression of phospho-Histone H2A.X (γH2A.X), a biomarker for DNA damage, cellular senescence, aging, and apoptosis [48]. Western blots performed with 30 µg of whole RPE cell extracts showed one γH2A.X-immunoreactive band around 15 kDa (Figure 4A). Blots of $CoCl_2$ stimulated or in an 0.1% O_2 atmosphere cultured cells produced a stronger immunoreactive signal, than those cultured in presence of high NaCl (Figure 4A,B). Furthermore, the amount of cell-free DNA was increased in RPE cells cultured in the presence of $CoCl_2$ or in a 0.1% O_2 atmosphere. The release of cell-free DNA was not altered by NaCl (Figure 4C). The results demonstrate that cellular stress caused by hypoxia may facilitate the release and accumulation of endogenous DNA fragments. High extracellular osmolarity only has a small non-significant effect on γH2A.X expression and no effect on the release of cell free DNA in cultured RPE cells.

Effects of TLR9 agonist on gene- and protein expression: To analyze the effects of viral/bacterial DNA, RPE cells were cultured in presence of a synthetic analog of viral/bacterial DNA (ODN 1826, 1 µM). The mRNA levels of TLR9 downstream signaling proteins such as the adaptor protein MYD88, and transcription factors like interferon regulatory factor (IRF)-7, and RELA (p65 subunit of NF-κB) were significantly induced by ODN 1826 (Figure 5B-D). Gene expression of proteins associated with inflammation or AMD like IFN-A (*IFNA*), cyclooxygenase-2 (*COX2*) were upregulated (Figure 5E,F) as well as matrix metalloproteinase 9 (*MMP9*; Figure 5J). TGF-β1 protein secretion (Figure 5K) was significantly increased after 24 h of stimulation, while *TGFB1* gene expression remained unchanged (Figure 5H). ODN 1826 had a slight effect on *VEGFA* after 6 h stimulation (Figure 5G), and no effect on *MMP2* mRNA (Figure 5I). Under the used conditions ODN 1826 had no significant effect on *TLR9* gene expression (Figure 5A). But we could show that the stimulation of cultured RPE cells with ODN 1826 induced the gene expression of different TLR9 downstream signaling

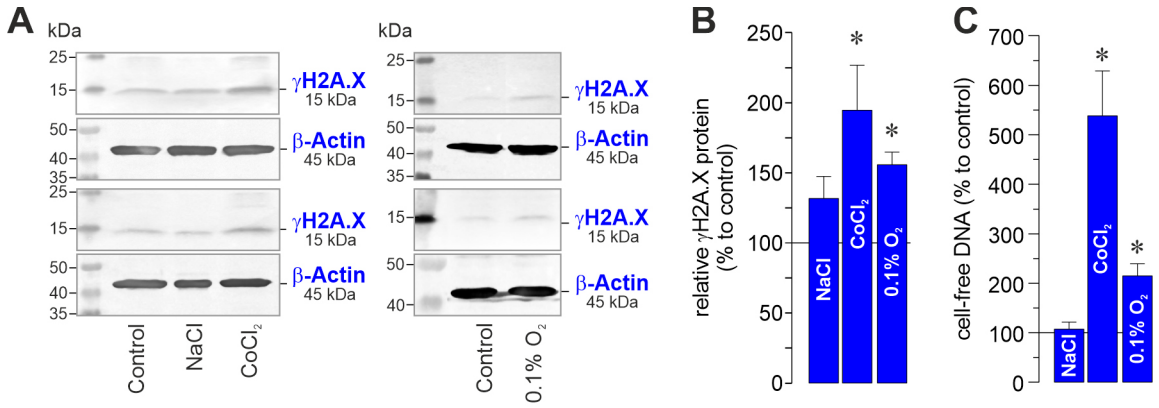

Figure 4. Expression of phosphorylated histone H2A.X (γH2A.X) protein in cultured human RPE cells. Cells were cultured in presence of $CoCl_2$ (150 µM), NaCl (+100 mM) or in a 0.1% O_2 atmosphere for 24 h. **A**: Representative western blots of γH2A.X protein using 30 µg whole cell protein extract. β-actin was used as loading control. The image shows two examples of 4 experiments. **B.** Signals quantified by densitometry and normalized with β-actin are shown in relation to the untreated control (100). **C**: The amount of cell-free DNA released from RPE cells that were cultured under hyperosmotic (+100 mM NaCl) as well as hypoxic conditions ($CoCl_2$, 0.1% O_2 atmosphere) for 24 h. The results are shown as a percentage of the untreated control group. (100). Each bar represents data from 4 (western blot) and 5 (cell-free DNA) independent experiments with cells from different donors. The statistical analysis was performed using the One-way ANOVA followed by Bonferroni's multiple comparison test. Significant difference *versus*. unstimulated control: *p<0.05. .

proteins and AMD associated proteins as well as the secretion of TGF-β1. This is an indication of the activating properties of ODN 1826 on TLR9 in RPE cells.

Effects of TLR9 blockade on gene expression: To investigate whether TLR9 activity influences the expression of different genes in RPE cells, we used two different inhibitory oligonucleotides specific to TLR9, iODN 2088 and iODN INH-18, in cells cultured under control, hyperosmotic, $CoCl_2$-simulated hypoxic conditions, and in a 0.1% O_2 atmosphere. As shown in Figure 6A, blockade of TLR9 activity had no effects on the *TLR9* gene expression under control conditions nor under simulated hypoxia. TLR9 blockade caused a downregulation under hypoxic condition in respect to various other genes: *MYD88* (Figure 6B), *IRF7* (Figure 6C), *RELA* (Figure 6D), *IFNA* (Figure 6E), *COX2* (Figure 6F), and *MMP9* (Figure 6G). The data suggest that activation of TLR9 contributes to the hypoxic gene expression of inflammatory factors in cultured RPE cells. Inhibition of TLR9 activity additionally reduced ($p<0.05$) the gene expression of *MYD88* (Figure 6B), *IRF7* (Figure 6C), and *COX2* (Figure 6G) under control conditions. TLR9 also seems to influence inflammatory processes under normoxia. No upregulation of *MYD88* was observed in RPE cells cultured for 24 h in a 0.1% O_2 atmosphere. This could be caused by the long duration of the stimulation. Under these conditions, *MYD88* mRNA expression was significantly increased at an early stage (2 h) and returned to control levels after 6 h (Appendix 4). The results of TLR9 activation with ODN 1826 supports the assumption that the regulation of *MYD88* is an early event (Figure 5B).

The TLR9 blockade did not change the expression of *VEGFA* (Appendix 5), and *TGFB1* (data not shown). VEGF-A protein secretion also remained unaffected (data not shown). But TGF-β1 protein secretion was significantly reduced by both TLR9 inhibitory oligonucleotides in RPE cells under control conditions, $CoCl_2$-simulated hypoxia, and 0.1% O_2. $CoCl_2$-induced hypoxia reduced the amount of secreted TGF-β1 under the used conditions. In contrast, TGF-β1 secretion was increased in RPE cells cultured under a 0.1% O_2 atmosphere. Both TLR9 inhibitory oligonucleotides significantly reduced TGF-β1 secretion under both hypoxia-simulated conditions (Figure 6H). These results indicate a role of active TLR9 in TGF-β1 protein secretion. This effect is confirmed by the results of the TLR9 agonist ODN 1826 (Figure 5K).

High extracellular osmolarity did not alter TLR9- and γH2A.X protein expression (Figure 3C, D; Figure 4A,B). Therefore, we used these conditions to examine only selected genes such as of *TLR9*, *RELA*, *TGFB1*, and *VEGF*. The TLR9 inhibition did not influence the expression of these genes under hyperosmotic conditions (Appendix 5) indicating that TLR9 activity may have no influence on the here analyzed genes under extracellular hyperosmolarity in RPE cells.

Different studies have shown that besides other signaling pathways, NF-κB is involved in the TLR9 response [49,50]. Studies on *RELA* mRNA expression suggest that TLR9 plays

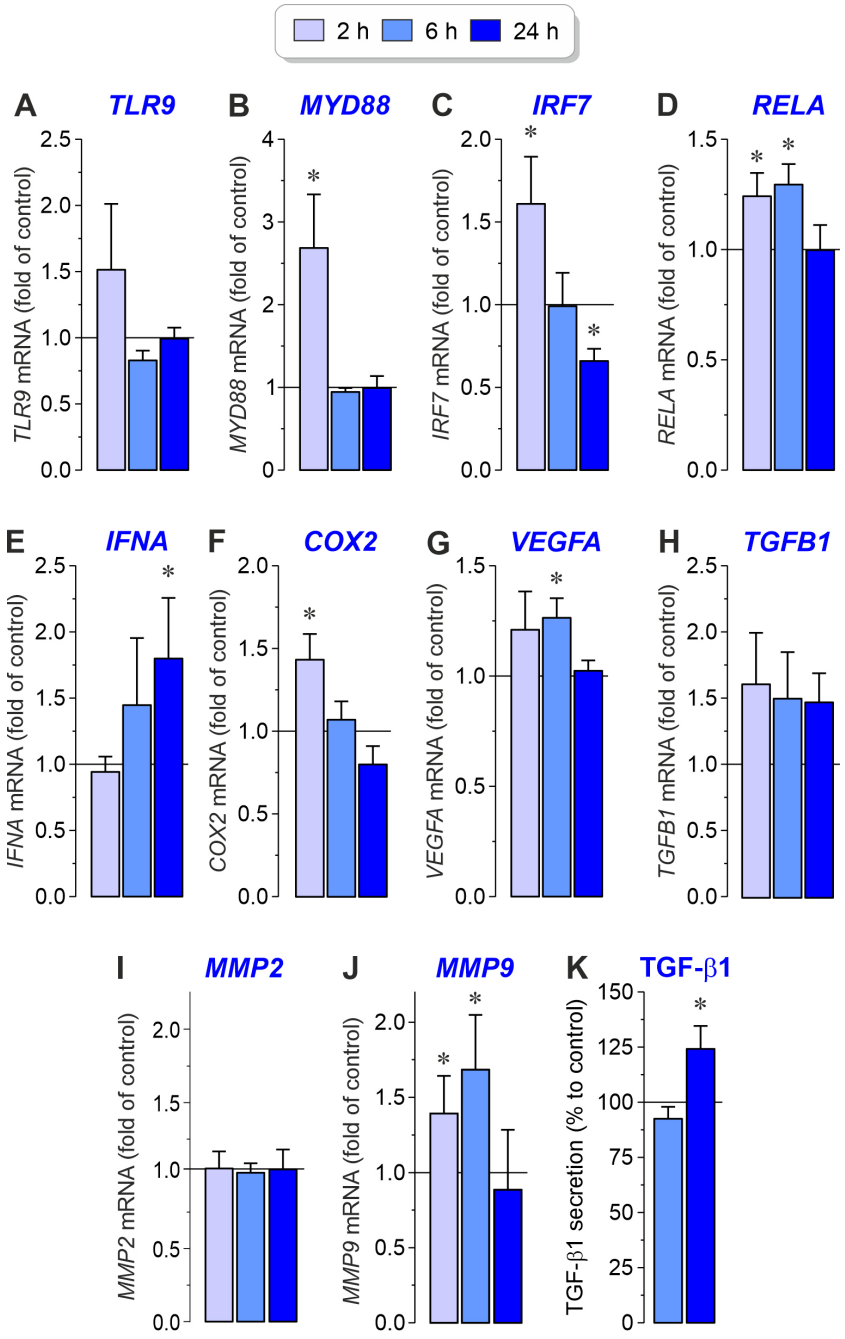

Figure 5. Effects of TLR9 agonist ODN 1826 on gene expression of TLR9 downstream signaling components and AMD associated proteins in RPE cells. RPE cells were cultured in presence of ODN 1826 (1 µM) for 2, 6 and 24 h. The mRNA amounts were examined with qPCR. Results are shown as fold changes to unstimulated controls. QPCR negative controls were performed with double-distilled water instead of cDNA. *ACTB* was used to normalize the results. Secreted TGF-β1 protein was analyzed in cell culture supernatants (24 h) using ELISA. The results are shown as percentage of the untreated control. The gene expression of the following factors was investigated: **A**: *TLR9* (n=4–5), **B**: TLR9 adaptor protein *MYD88* (n=4–5), **C**: transcription factor *IRF7* (n=4–6), **D**: transcription factor *RELA* (the gene of p65 subunit of transcription factor NF-κB, n=5), **E**: *IFNA* (n=5–6), **F**: *COX2* (n=6), **G**: *VEGFA* (n=5–6), **H**: *TGFB1* (n=6), **I**: *MMP2* (n=4), and **J**: *MMP9* (n=4). **K**: The protein secretion of TGF-β1 (n=3) is presented. Each bar (mean ± SEM) shows results from independent experiments using RPE cells from different human eye donors. Mann–Whitney-U-Test was used for statistical analysis of the qPCR results. One-way ANOVA followed by Bonferroni's multiple comparison test was used to analyze the ELISA-results. Significant difference *versus*. unstimulated controls: *p<0.05.

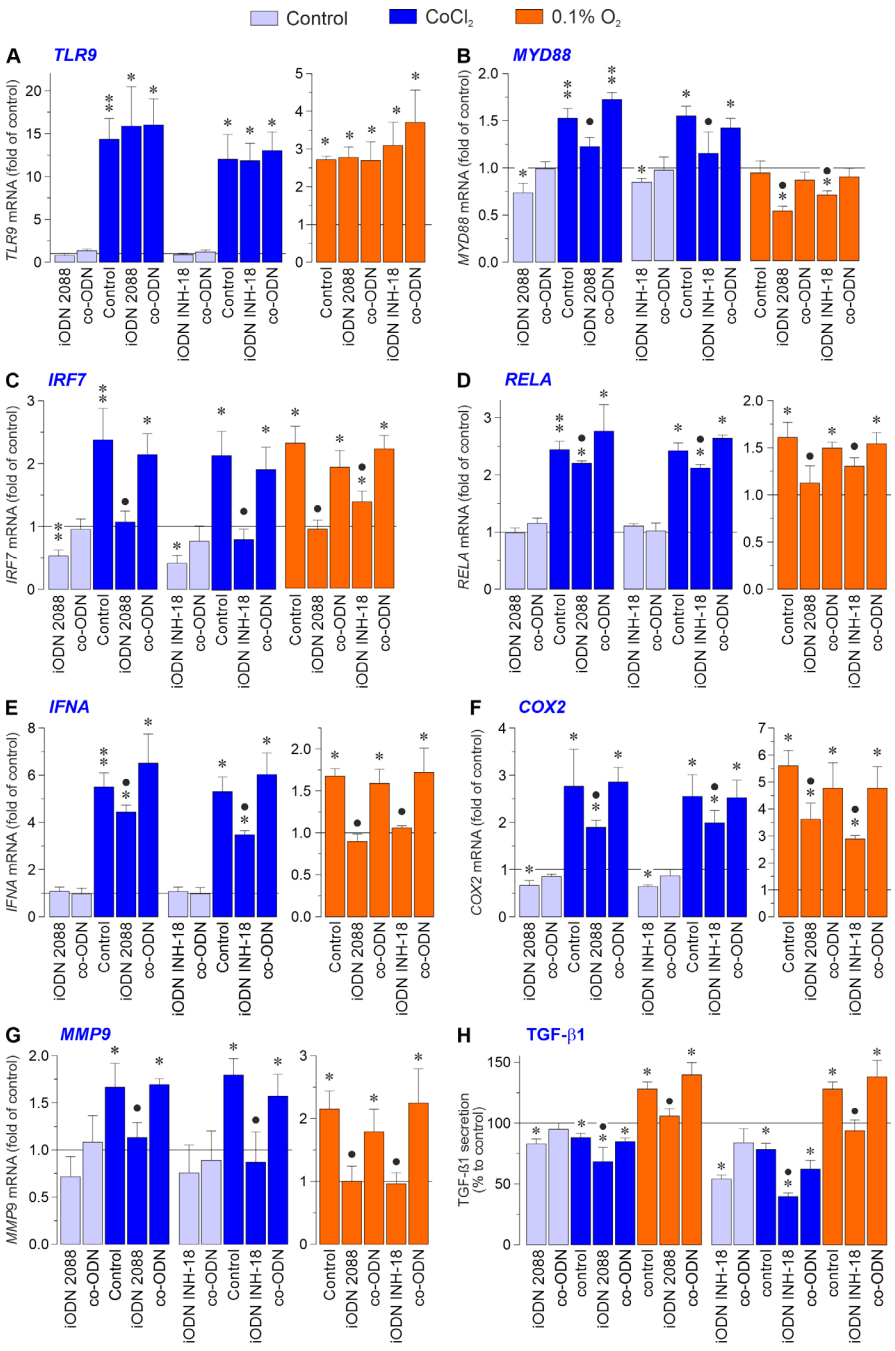

Figure 6. Effects of inhibitory oligonucleotides for TLR9 on the hypoxic gene and protein expression in cultured human RPE cells. The cells were stimulated for 24 h with $CoCl_2$ (150 µM) or in 0.1% O_2 atmosphere as indicated by the panels of the bars. TLR9 was blocked by iODN 2088 (1 µM) or iODN INH-18 (2.5 µM). As negative control, control co-ODN 2088 (co-ODN; 1 and 2.5 µM) was used. Results are shown as fold change to unstimulated controls (1). TGF-β1 protein secretion was analyzed in cell culture supernatants using ELISA. Results are shown as per cent to $CoCl_2$ or to 0.1% O_2 controls (100). The gene expression of **A**: *TLR9* **B**: TLR9 adaptor protein *MYD88*. **C**: Transcription factor *IRF7*. **D**: Transcription factor *RELA* (the gene of p65 subunit of transcription factor NF-κB). **E**: *IFNA*, **F**: *COX2*, **G**: *MMP9*. The data are shown as fold change of unstimulated control (1). *ACTB* and *B2M* were used to normalize the results. **H**: Shows total TGF-β1 protein amounts secreted by RPE cells cultured in presence of $CoCl_2$ or a 0.1% O_2 atmosphere. Each bar represents data (mean ± SEM) obtained in 4–7 (iODN 2088) or 3–4 (iODN INH-18) independent experiments using cells from different donors. Mann–Whitney-U-Test was used for statistical analysis. Significant difference versus unstimulated control: *p<0.05, **p<0.01. Significant differences versus $CoCl_2$ or O.1% O_2 controls: ●p<0.05. .

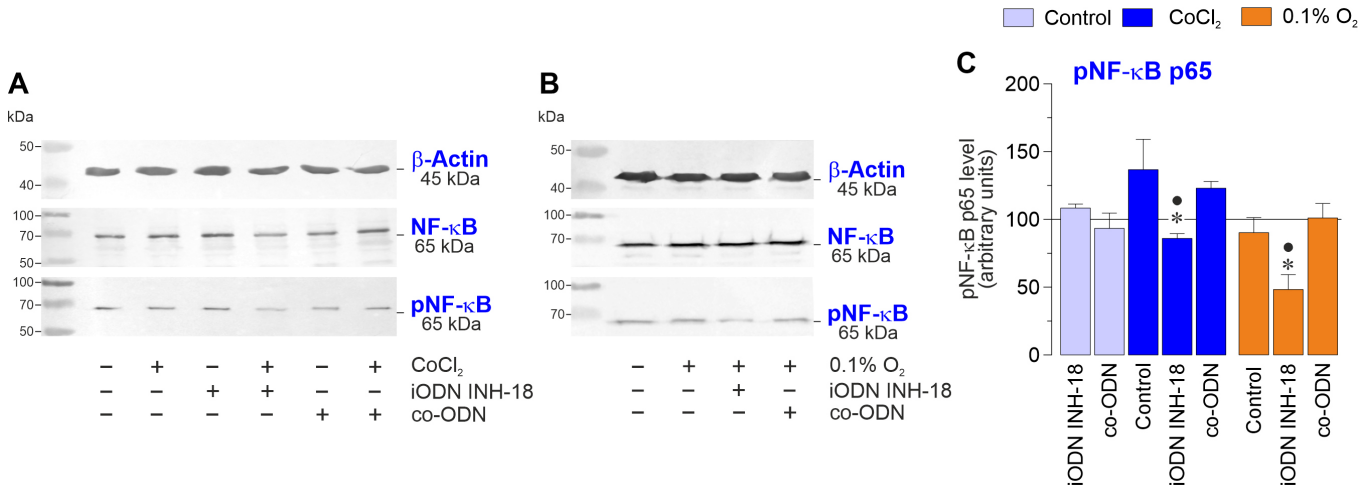

Figure 7. Effects of the TLR9 inhibiting oligonucleotide iODN INH-18 on the activation of NF-κB under chemical hypoxia (150 µM $CoCl_2$) or 0.1% O_2 atmosphere in human RPE cells TLR9 was blocked with iODN INH-18 (2.5 µM). The cells were cultured for 24 h in normoxic or hypoxic conditions ($CoCl_2$, 0.1% O_2 atmosphere) as indicated by the panels of the bars. The level of total proteins and phosphorylated proteins were determined with western blotting. As negative control co-ODN 2088 (co-ODN; 2.5 µM) was used. **A**, **B**: Representative western blots of different total and phosphorylated signaling proteins using 25 µg whole cell protein extract for total protein and 35 µg for phosphorylated proteins. β-actin was used as loading control. The image shows one example of 3 experiments. **C**. Graphical illustration of western blotting results of phospho-NF-κB p65 (pNF-κB p65) are presented. Signals quantified by densitometry and normalized with β-actin are shown in relation to the untreated control (100). Each bar represents data from 3 independent experiments with cells from different donors. One-way ANOVA followed by Bonferroni's multiple comparison test was used to analyze the results Significant difference *versus*. unstimulated control: *p<0.05. Significant differences versus $CoCl_2$ or 0.1% O_2 controls: ●p<0.05. .

a role in this process. Therefore, the effects of blocking TLR9 with iODN INH-18 on the activation of NF-κB was included in the investigations. Activation of the signal protein was determined by western blotting. Hypoxia ($CoCl_2$, 0.1% O_2) had no effect on NF-κB baseline activation (Figure 7) after 24 h stimulation. Under these conditions TLR9 antagonist iODN INH-18 significantly reduced the amount of pNF-κB in RPE cells below the baseline level.

RPE cell viability: To analyze whether TLR9 activity influences cellular properties we tested both inhibitory oligonucleotides specific to TLR9, iODN 2088 and iODN INH-18, in cells cultured under control, high extracellular osmolarity (+100 mM NaCl), $CoCl_2$-simulated hypoxic conditions, and in an 0.1% O_2 atmosphere. We found that adding of 100 mM NaCl to the culture medium did not alter the RPE cell viability whereas addition of 150 µM $CoCl_2$ or a reduced oxygen content significantly decreased ($p<0.05$) the viability (Figure 8A,B). This reduced cell viability may be caused by an increased necrosis and apoptosis of the cells (Figure 8C) under both hypoxic conditions. Coaddition of the inhibitory oligonucleotides (iODN) specific to TLR9, iODN 2088 (Figure 8A) or iODN INH-18 (Figure 8B), had no effect on the viability under control, hyperosmotic conditions, and in $CoCl_2$ induced hypoxia. Coaddition of the inhibitory oligonucleotides significantly reduced the viability of cells cultured in an 0.1% O_2 atmosphere. This could indicate a protective effect by TLR9 under these conditions. Administration of iODNs had no effects on the proliferation rate of the cells under the three conditions tested either (data not shown).

Role of TGF-β1: It is known that hypoxic conditions alter the gene expression of different cytokines including *TGFB1* [43,51]. An increase of TGF-β1 in patients with nAMD has been described [35]. Besides the canonical TGF-β signaling via Smad proteins there is a non-canonical TGF-β signaling which includes signaling proteins like ERK1/2, p38 MAPK, PI3K or JNK [32]. We found, that TGF-β1 significantly reduced the *TLR9* mRNA and protein expression in RPE cells under normoxic conditions (Figure 2G; Figure 3C,D, Figure 9A,D), same as under $CoCl_2$-induced chemical hypoxia and in a 0.1% O_2 atmosphere (Figure 9B,C). Therefore, potential pathways involved in the autocrin/paracrin TGF-β1 signaling were investigated. Pharmacological inhibitors were used to block the activation of signaling proteins and thus identify mediating signal pathways. Under control conditions the *TLR9* mRNA amount was increased significantly by blocking the activation of p38 MAPK, (SB2035580), and JNK (SP600125; Figure 9A). The *TLR9* mRNA reducing effect of TGF-β1 was reversed with an anti TGF-β pan specific

neutralizing antibody (aTGF-β ab). This may indicate a function of these signaling proteins in inhibiting the *TLR9* gene expression under normoxia. Blocking TGF-β1-signaling with SB431542 or SIS3 increased the $CoCl_2$-induced *TLR9* mRNA amount significantly compared to the $CoCl_2$ control, whereas the increase induced by the anti-TGF-β pan-specific neutralizing antibody was not significant under these conditions. Inhibition of p38 MAPK or JNK significantly increased the $CoCl_2$-induced *TLR9* gene expression compared to the $CoCl_2$ control while inhibition of ERK1/2 (PD98059) and PI3-kinase (LY294002) had no effect. With a few exceptions, these results were confirmed with RPE cells cultivated in a 0.1% O_2 atmosphere. Here, the increase in *TLR9* gene expression due to the effect of the neutralizing TGF-β1 antibody was significant. In contrast to the $CoCl_2$ results, blocking PI3-kinase increased the *TLR9* mRNA and the CREB inhibitor had no effect here. Thus, our results may indicate a contribution of TGF-β signaling to decrease the *TLR9* expression under normoxia and chemical hypoxia as well as in a reduced O_2 environment in cultured RPE cells.

To confirm these results and to specify the role of TGF-β1 signaling, RPE cells were additionally co-incubated in the presence of TGF-β1 (10 ng/ml) and the pharmacological inhibitors for 24 h (Figure 9D). Under these conditions the inhibitory effect of TGF-β1 on the *TLR9* gene expression was reversed by an anti TGF-β pan specific neutralizing antibody, by blocking of TGF-β1 superfamily activin receptor-like kinase receptors, transcription factors Smad3, as well as by p38 MAPK, JNK, and PI3K. Inhibition of ERK1/2 or CREB had no effect. These results may support the function of TGF-β1 in reducing *TLR9* expression.

DISCUSSION

Selected TLRs in the retina play key roles in the development of retinal ischemic diseases including ischemia-reperfusion injury, glaucoma, AMD, and diabetic retinopathy [52-54]. TLRs can be expressed by multiple retinal cell types such as glial, RPE, and photoreceptor cells [54]. In the present study, we investigated the expression of *TLR* genes in acutely isolated and cultured human RPE cells. We found that acutely isolated RPE cells express the mRNA of all 10 TLRs, whereas cultured RPE cells lacked detectable transcripts of *TLR7*, *8* and *10*. Kumar et al. [24] identified all *TLR*s except *TLR8*. The discrepancy with our findings may result from differences in culture conditions. *TLR1*, *2*, *5*, and *9* mRNA amounts were significantly higher in acute RPE cells compared to cultured

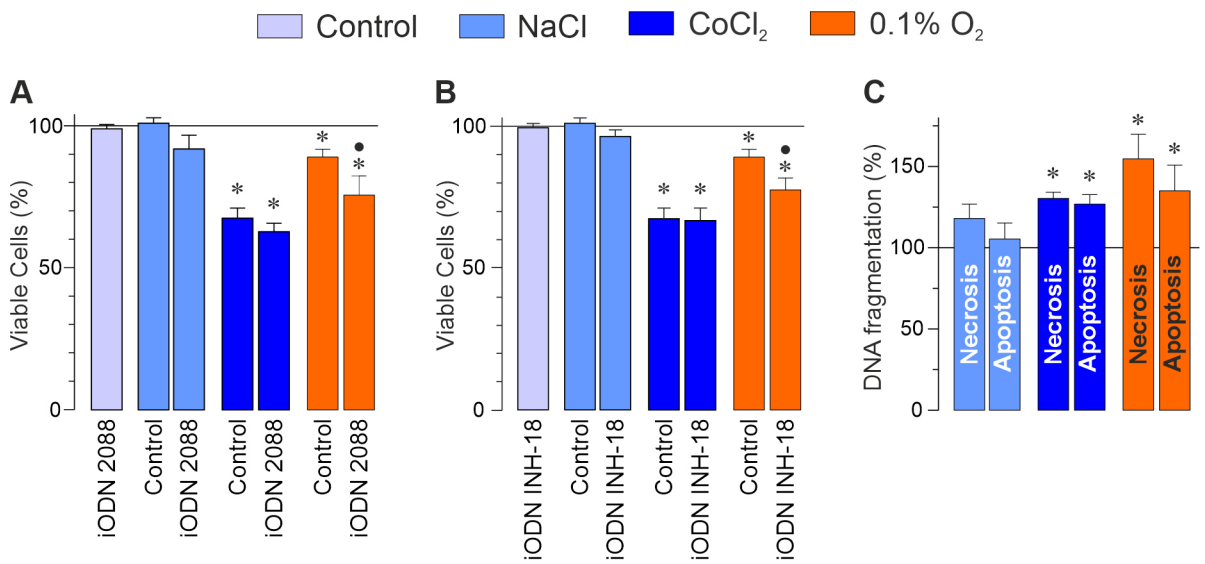

Figure 8. Effects of TLR9 inhibiting oligonucleotides on the viability of cultured human RPE cells under hyperosmotic conditions and hypoxic conditions ($CoCl_2$, 0.1% O_2). The cells were cultured 24 h in absence and presence of high NaCl (+100 mM), $CoCl_2$ (150 µM), as well as 0.1% O_2 with and without inhibitory oligonucleotides specific to TLR9. **A**: Effect of the inhibitory oligonucleotide iODN 2088 (1 µM) on the viability of cultured RPE cells. n=7 (NaCl), n=6 ($CoCl_2$), and n=4 (0.1% O_2). **B**: Effect of the TLR9 inhibitory oligonucleotide iODN INH-18 (2.5 µM) on the viability of cultured RPE cells (n=6 for NaCl and $CoCl_2$), and n=4 (0.1% O_2). **C:** Influence of chemical hypoxia induced by $CoCl_2$, of a 0.1% O_2 atmosphere or of high extracellular osmolarity on necrosis and apoptosis in cultured RPE cells (n=4). The data are shown as percent of unstimulated control (100%). Each bar represents data obtained in independent experiments using cells from different donors. Mann–Whitney-U-Test was used for statistical analysis. Significant difference versus unstimulated control: *p<0.05. Significant differences *versus* 0.1% O_2 controls: ●p<0.05. .

cells, as indicated by lower PCR cycle numbers (Figure 1B). The reason for these differences is not clear, but may be due

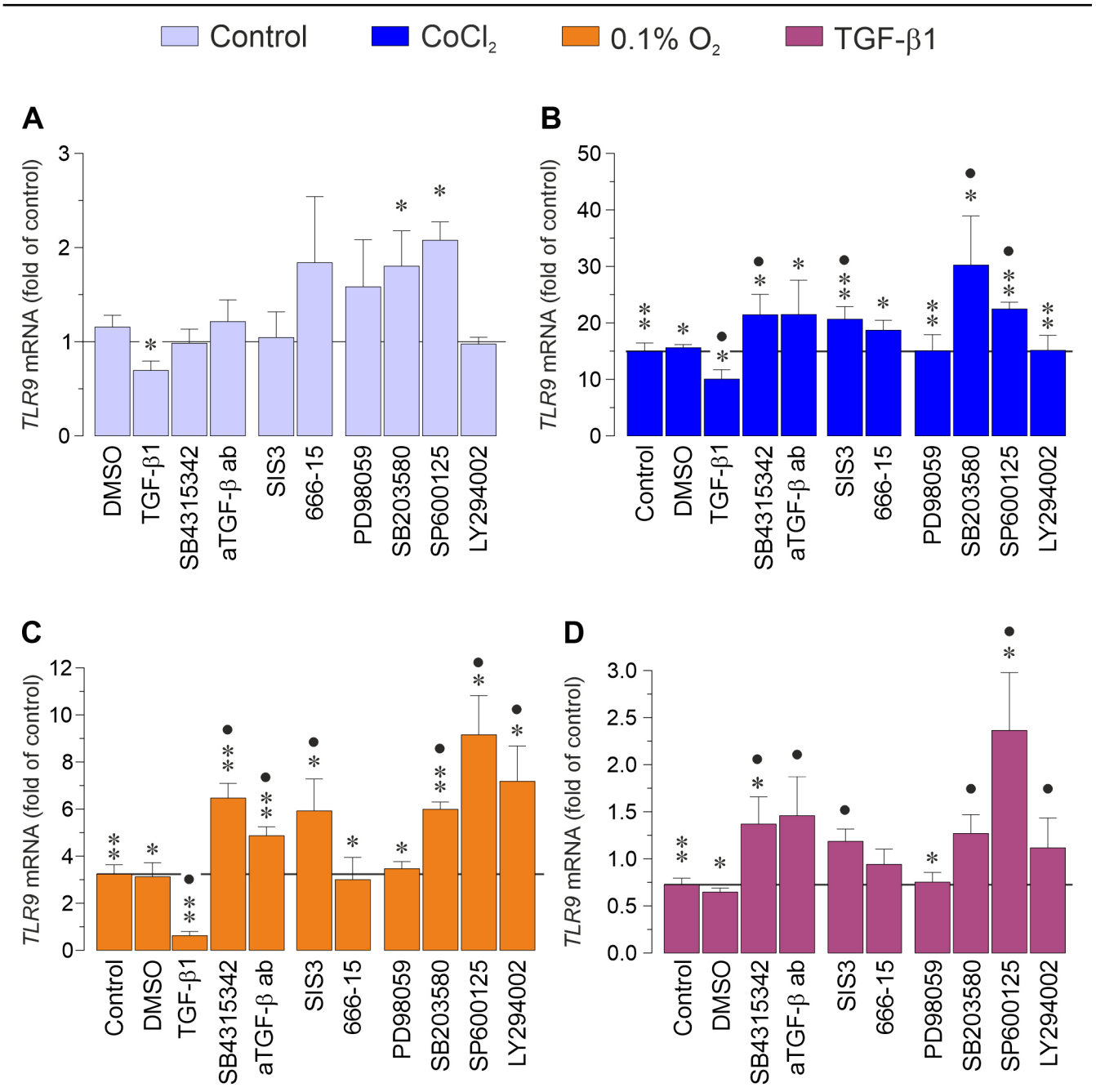

Figure 9. Cellular signaling mediating the reducing effect of TGF-β1 on the *TLR9* expression in cultured RPE cells. The *TLR9* gene expression was determined with qPCR in RPE cells cultured in absence or presence of hypoxia mimetic $CoCl_2$ (150 µM), respectively (**A, B**), in a 0.1% O_2 atmosphere (**C**) or in presence of TGF-β1 (10 ng/ml; **D**) for 24 h. The RPE cells were pre-incubated with the inhibitors for 30 min. The following inhibitors were used: the inhibitor of TGF-β1 superfamily activin receptor-like kinase receptors, SB431542 (10 µM), an anti TGF-β pan specific neutralizing antibody (10 µg/ml), the Smad3 inhibitor, SIS3 (10 µM), the CREB inhibitor 666–15 (250 nM), the ERK1/2 inhibitor, PD98059 (20 µM), the p38 MAPK inhibitor, SB203580 (10 µM), the JNK inhibitor SP600125 (10 µM), the inhibitor of PI3K-kinases, LY294002 (5 µM). DMSO (1:1000) served as solvent for the inhibitors. The data are displayed as fold change of unstimulated control (1). *ACTB* and *B2M* were used to normalize the results. Each bar shows data obtained from 3 to 6 independent experiments with cells from different donors. One sample *t* test was used for statistical analysis. Significant difference versus unstimulated control: *p<0.05; **p<0.01. Significant differences versus $CoCl_2$ control (**B**), versus 0.1% O_2 (**C**) or versus TGF-β1 control (D): ●p<0.05. .

to activation of RPE cells during the isolation procedure from the donor eyes.

The regulation of *TLR* gene expression was analyzed in human RPE cells cultured under simulated pathological conditions including hypoxia ($CoCl_2$, 0.1% O_2), high extracellular osmolarity (+100 mM NaCl, +200 mM sucrose), retinal disorders-associated growth factors (VEGF, TGF-β1), or blood-derived components (serum, thrombin). Both simulated types of hypoxia significantly increased *TLR9* expression whereas *TLR3* mRNA was downregulated. *TLR2* was upregulated only in RPE cells cultured in a 0.1% O_2 atmosphere and *TLR4* was upregulated only by $CoCl_2$. The reason for this discrepancy is unclear, but could be related to the potentially stronger stress effect of $CoCl_2$, which does not fully mimic hypoxic conditions.

Extracellular hyperosmolarity enhanced the mRNA amount of *TLR1*, *4*, *6,* and *9* with the strongest effect on *TLR9.* These results show that *TLR9* mRNA was most strongly regulated (Figure 2) and may confirm a function against invading viruses and bacteria as well as DAMPs. Triamcinolone acetonide significantly increased the *TLR9* gene expression, while serum, thrombin, and TGF-β1 suppressed it. VEGF-A had no significant effect. VEGF-A is associated with compromise of the blood-retina-barrier in nAMD and diabetic retinopathy, allowing infiltration of blood-derived components [55]. Thus, VEGF-A might indirectly influence *TLR9* expression by modulating barrier permeability. The elevated *TLR9* mRNA level under hyperosmotic conditions (Figure 2C,D) suggests a role for TLR9 in sensing osmotic stress in RPE cells.

The effects of $CoCl_2$, 0.1% O_2, TGF-β1 or triamcinolone acetonide on *TLR9* mRNA were validated at the protein level; however, NaCl did not alter protein levels (Figure 3C,D). The corticosteroid triamcinolone acetonide is clinically employed to treat macular edema in various retinopathies [56]. Although triamcinolone acetonide has been increasingly replaced by anti-VEGF drugs, combination therapy with triamcinolone may provide enhanced efficacy [47]. However, in our in vitro study, triamcinolone induced TLR9 expression. Rare ocular side effects of intravitreal triamcinolone, including sterile endophthalmitis, have been reported [57], typically attributed to preservatives and usually resolve within one to two weeks [58]. But our in vitro finding is not sufficient to make a recommendation for clinical practice because upregulation of a single pro-inflammatory receptor is not equal to the net pro-inflammatory effect of the drug.

In addition to TLR3, 7, and 8, TLR9 is mainly located within intracellular membranes, including endosomes, lysosomes, and endoplasmic reticulum [16]. This was confirmed for TLR9 in our study on cultured RPE cells. Immunocytochemical staining demonstrated strong intracellular TLR9 immunoreactivity with weak membrane localization (Figure 3A). Using immunoblot analyses, TLR9 protein was detected in membrane-enriched protein fractions consistent with localization to intracellular organelles (Figure 3B). These results are confirmed by flow cytometric analysis of Ebihara et al. [25].

TLR9 recognizes DNA fragments containing unmethylated CpG-DNA released by proliferating and dying microbes, and by mitochondria derived from degraded cells [18-20,23]. Mitochondrial or nuclear damage under conditions of cellular stress is associated with the release of genetic material into the cytosol [20,59]. Mitochondrial DNA (mtDNA), which predominantly contains CpG-motifs, activates TLR9 in macrophages and contributes to inflammatory responses. MtDNA acts as a key DAMP and triggers various inflammatory and degenerative diseases [20]. In hepatocytes, accelerated non-apoptotic cell death has been observed following activation of TLR9/IFN-β signaling by mtDNA [23]. RPE cells are also exposed to blood-borne DAMPs. It was shown that systemic exposure to the TLR9 ligand CpG-ODN causes widespread ocular inflammation, including increased macrophage accumulation of macrophages in the subretinal space [60].

In the aged retina systemic infection can aggravate AMD, which is associated with a chronic inflammation, an important factor of necrosis, and is accompanied by the release of DAMPs [14]. The formation of γH2A.X is a fast reaction to cellular DNA damage and serves as a marker for cellular senescence and apoptosis [48]. γH2A.X protein levels were elevated in cultured RPE cells under $CoCl_2$-induced hypoxia as well as under a 0.1% O_2 atmosphere (Figure 4A,B). Thus, hypoxia induced both apoptosis and necrosis in RPE cells (Figure 8C) [61], which may contribute to the release of DNA fragments (Figure 4C). An increased release of DNA fragments by RPE cells due to hypoxia was detected with $CoCl_2$-induced hypoxia having a stronger effect (Figure 4C). Hyperosmotic conditions did not alter γH2A.X protein expression (Figure 4A,B), cell viability, apoptosis and necrosis (Figure 8), or DNA release (Figure 4C). The results demonstrate that cellular stress caused by hypoxia may facilitate the release and accumulation of endogenous DNA fragments. Thus, self-derived DNA may serve as an endogenous ligand for activation of intracellular located TLRs, potentially promoting cellular failure.

Among the intracellularly localized TLRs, *TLR7* and *TLR8* mRNA were not detectable in this study, and *TLR3* expression was reduced by hypoxia. Only TLR9 mRNA was

significantly upregulated under hypoxia ($CoCl_2$, 0.1% O_2), which was confirmed at the protein level. This may highlight the importance of TLR9 as a unique sensor for DNA fragments with unmethylated CpG-DNA motifs in cultured human RPE cells mainly under hypoxic conditions, and was the reason for investigating the function of TLR9.

The TLR9 agonist ODN 1826 has been shown to strongly promote pro-inflammatory activation of macrophages [62]. Activation of TLRs, e.g., TLR9, enhances bacterial phagocytotic capacity in RPE cells via p38 MAPK-dependent gene expression changes [49]. ODN 1826 only had an early modest effect on TLR9 gene expression in cultured RPE cells (Figure 5A). Accordingly, activation of TLR9 has no regulatory effect on its own mRNA expression. Similar results were reported using ODN 2006, another class B CpG-ODN TLR9 ligand [27]. The authors ruled out insufficient CpG-ODN concentration as a cause by demonstrating its effects on the expression of various downstream genes. We found that cultivation of human RPE cells cultured in the presence of ODN 1826 showed a significant increase in the gene expression of TLR9 signaling-associated proteins, including adaptor *MYD88*, transcription factors *IRF7, RELA,* inflammatory factors, *IFNA, COX2,* matrix metalloproteinase *MMP9,* and the angiogenic growth factor *VEGFA* (Figure 5) confirming the findings of Brosig et al. [27], and demonstrating the activation of TLR9 by ODN 1826.

In addition, TLR9 activity was blocked using two distinct inhibitory oligonucleotides, to examine its role in regulating the expression of inflammatory and pro-angiogenic genes. TLR9 blockade had no effect on *TLR9* mRNA levels under hypoxic conditions (Figure 6A) conforming the ODN 1826 results. Blocking of TLR9 decreased the gene expression of adaptor protein *MYD88,* transcription factor *IRF7*, and inflammatory mediator *COX2* under both control and hypoxic conditions (Figure 6B,C,F), whereas *RELA* (encoding NF-κB p65), *IFNA* and *MMP9* mRNA levels were reduced exclusively under hypoxia (Figure 6D,E,G). The inhibitory effect under normoxic conditions may indicate basic activation of TLR9, possibly due to the release of DNA from cells damaged by the cell culture method used.

No *MYD88* mRNA induction was detected after 24 h at 0.1% O_2. This may be caused by the long duration of stimulation. *MYD88* mRNA expression was significantly increased at an early stage (2 h) and returned to control levels after 6 h (Appendix 4). This finding is supported by the results obtained with ODN 1826 (Figure 5B).

In autoimmune diseases such as systemic lupus erythematosus and rheumatoid arthritis, TLR9 activates IRFs and/or NF-κB, resulting in enhanced production of interferons and cytokines, thereby amplifying inflammatory responses [16,21,22]. TLR9 induces p38 MAPK phosphorylation followed by NF-κB activation, thus promoting inflammation [62,63]. Hypoxic conditions did not alter the baseline level of phosphorylated NF-κB after 24 h. Inhibition of TLR9 lowered phosphorylation of NF-κB below this baseline level. Thus, TLR9 appears to be involved in maintaining a basal activation of NF-κB under normoxia and under hypoxic conditions.

Kawai and Akira [64] highlight the regulatory roles of IRF7, AP-1, and NF-κB in controlling the expression of type I interferons and other pro-inflammatory cytokines. Blocking TLR9 activity in cultured RPE cells attenuated the expression of inflammatory genes (*IFNA, COX2*) under both hypoxic conditions (Figure 6E,F). TLR9 activation may therefore promote inflammatory responses during retinal hypoxia. The angiogenic factor *VEGFA* mRNA (Appendix 5) and VEGF-A protein secretion (data not shown) remained unchanged. Similar results regarding to the *VEGF* mRNA were reported by Brosig et al. [27] using ODN 2006 another TLR9 agonist. The lack of influence of TLR9 on VEGF expression in RPE cells suggests that TLR9 does not directly promote VEGF-induced pathological angiogenesis. An indirect effect due to the TLR9-increased secretion of TGF-β1 and the subsequent induction of VEGF-A [34] would be entirely possible.

The underlying cause of the selective inhibitory effects of TLR9-blocking oligonucleotides under hypoxic conditions remains unclear. We observed that high NaCl did not affect the viability of cultured RPE cells, whereas $CoCl_2$-induced hypoxia or a 0.1% O_2 atmosphere significantly reduced cell viability, with a stronger effect of $CoCl_2$ and triggered both apoptosis and necrosis (Figure 8) [61]. Since loss of cell viability is accompanied by cellular breakdown, it is plausible that fragments of mitochondrial DNA and nuclear proteins are released and act as DAMPs. This was demonstrated by increased levels of cell-free DNA only in hypoxia (Figure 4C). These DAMPs may activate TLR9 in surviving cells, thereby intensifying sterile inflammation. In retinal diseases characterized by tissue destruction, elevated local and/or systemic DAMP levels can trigger or sustain both local and systemic inflammation.

TLR9 stimulation by DAMPs, upregulates inflammatory genes such as *IFNA,* and *COX2,* partly via NF-κB, may contribute to hypoxia-induced retinal tissue degeneration. However, since TLR9-inhibitory oligonucleotides only partially suppressed the hypoxia-induced expression of inflammatory genes (Figure 6E,F) it is likely that additional signaling pathways - beyond those examined - are involved. Such pathways may include TLR7, which detects single-stranded RNA, TLR8, which recognizes viral single-stranded

RNA, or TLR3 which detects double-stranded RNA. Activation of TLR2, 3, and 4 reduces RPE function and mediates RPE cell degeneration, which may contribute to development or aggravation of AMD and may involve in the immune response within the retina [24,28]. Viral activation of TLR2 in RPE cells has been shown to promote choroidal neovascularization in experimental models [26]. The present findings suggest that, alongside other TLR subtypes, TLR9 in RPE cells may facilitate retinal inflammation under necrotic conditions, such as in geographic atrophy, typical for dry AMD. Since our investigations are mainly limited to the gene expression of TLRs under various conditions, further studies on TLR protein expression are necessary to better understand their specific functions. Conversely, since IFN-β suppresses the expression of inflammatory chemokines and adhesion molecules in the retina, TLR signaling in RPE cells may also serve an immuno-suppressive function, helping to limit excessive inflammation [65]. However, beside pro-inflammatory effect we observed no influence on $CoCl_2$-reduced viability but an additional decrease in viability due to the inhibitory oligonucleotides in RPE cells cultured in a 0.1% O_2 atmosphere (Figure 8A,B), suggesting a protective effect of TLR9 under hypoxic conditions. The downstream effects of TLR9 signaling in RPE cells require further examination in animal models.

TGF-β1 significantly downregulated TLR9 expression (Figure 2G, Figure 3C,D). TGF-β1, a member of the multifunctional transforming growth factor superfamily, exhibits context-dependent and sometimes contradictory roles in neovascular AMD. It has been associated with angiogenesis via *VEGFA*-induction [34] and with anti-inflammatory activity [37]. In animal models, TGF-β1 function appears to vary depending on the stage of nAMD, showing pro-angiogenic effects in acute or late stages and anti-angiogenic effects during early disease [33]. Carmeliet [66] describes a dose-dependent function of TGF-β1, with low concentrations promoting angiogenic factor expression and high concentrations inhibiting endothelial cell growth. Blockade of TGF-β1 signaling in TGF-β1 null mice resulted in early mortality due to multifocal inflammation [67]. Here we demonstrated that extracellular TGF-β1 suppressed *TLR9* mRNA expression under normoxia (Figure 2G) and reduced the TLR9 protein synthesis (Figure 3C,D) in cultured human RPE cells. This downregulation of *TLR9* mRNA was also observed under $CoCl_2$-induced hypoxic conditions as well as in a 0.1% O_2 atmosphere (Figure 9B,C). Blocking TGF-β superfamily activin receptor-like kinase signaling increased *TLR9* mRNA levels under both hypoxic conditions (Figure 9B,C), supporting the suppressive role of active TGF-β1. This effect was confirmed using a neutralizing pan-specific TGF-β antibody. We demonstrated that both, canonical (Smad 3-mediated) and non-canonical signaling pathways involving p38 MAPK, JNK, and PI3K contribute to *TLR9* mRNA downregulation (Figure 10). It should be noted that in $CoCl_2$-induced hypoxia, no significant effect of the neutralizing pan-specific TGF-β antibody and LY294002 was observed compared to 0.1% O_2. This could be due to possible stronger "pseudo-hypoxic" effects of $CoCl_2$.

The TLR9 agonist ODN 1826 increased TGF-β1 secretion from cultured RPE cells (Figure 5K). Blocking TLR9 activation by iODNs significantly reduced TGF-β1 secretion compared to the unstimulated control or both hypoxia controls (Figure 6H), indicating that active TLR9 promotes TGF-β1 release. However, *TGFB1* mRNA expression remained unchanged after treatment with ODN 1826 (Figure 5H) or iODNs (data not shown). One possible explanation is a compensatory downregulation of *TGFB1* transcription in response to elevated protein levels. Furthermore, TLR9 is involved in the activation of matrix metalloproteinases (MMPs) [68], which may subsequently activate latent TGF-β1 [30]. We found that activation of TLR9 with ODN 1826 significantly induced the *MMP9* gene expression (Figure 5J) whereas *MMP2* mRNA (Figure 5I) remains unaltered. Naik et al. [69] confirm these results with studies on ARPE-19 cells infected with multidrug-resistant (MDR-PA) clinical isolates of *Pseudomonas aeruginosa*. Blocking TLR9 activation reduced the hypoxia induced *MMP9* expression (Figure 6G) and may confirm the role of TLR9 in *MMP9* expression. Thus, active TLR9 likely contributes to both the secretion and activation of TGF-β1 via induction of *MMP9* expression in cultured RPE cells. This suggests a negative feedback loop whereby TLR9 activity suppresses its own expression through TGF-β1 induction. Besides TGF-β1 secreted by RPE cells, increased TGF-β1 levels have been reported in the vitreous, aqueous humor, and RPE/choroid interface of patients with nAMD, which may also modulate TLR9 expression in RPE cells [35,70]. According to our findings, autocrine and paracrine TGF-β1 may help limit retinal inflammation by downregulating TLR9 expression. This anti-inflammatory effect may result not only from direct transcriptional suppression of *TLR9*, as shown here, but also from inhibition of TLR9 signaling pathways. Naiki and colleagues [37] reported that TGF-β1 stimulates ubiquitination of the TLR adaptor protein MYD88, leading to its degradation and reduced intracellular levels, thereby dampening inflammation. They also observed that TGF-β1 attenuates the TLR9-mediated immune response by reducing CpG-DNA-induced type I interferon production via TRAF6 ubiquitination and inhibition of IRF7 phosphorylation [71].

TGF-β blockade has been proposed as a therapeutic strategy for nAMD due to its VEGF-inducing effect [33]. However, our findings call this approach into question, given the dual and context-dependent effects of TGF-β.

Our investigation has certain limitations. We employed cultured human RPE cells in vitro, which may not completely replicate in vivo physiology. Further research, including animal models, is needed to clarify the functional roles of TLR9 and TGF-β signaling in RPE dysfunction and AMD pathogenesis. The exclusive TLR9 focus is justified but perhaps overstated given *TLR2* upregulation under true hypoxia.

The study focuses primarily on changes in mRNA expression of various genes following activation (ODN 1826) or inhibition (ODN 2088, ODN INH-18) of TLR9. To elucidate the functional significance of TLR9, further investigations, e.g., with regard to cytokine production, are necessary to confirm the mRNA results and demonstrate the role of TLR9 in immunological processes in RPE cells. The feedback loop remains mechanistically incomplete without MMP-9 inhibitor experiments or active TGF-β1 measurements. The loading controls for original western blots ($CoCl_2$ stimulation) remain unverifiable.

Here, the effects of $CoCl_2$-induced hypoxia and reduced O_2 content were directly compared. The results obtained with $CoCl_2$ should be interpreted with caution because $CoCl_2$ chemically stabilize HIF-1α by competing with Fe^{2+} ions which activate HIF-prolyl hydroxylases (PHD) but does not affect pericellular oxygen level, and may cause stress and cytotoxic effects [72]. Nevertheless, our results show that the use of $CoCl_2$ as a hypoxia mimetic in RPE cells is entirely possible but careful control and cautious interpretation of the data are required.

In summary, our data suggest that TLR9 stimulation may drive local inflammation in damaged retinal tissue, such as that induced by hypoxia. Such stimuli may include mitochondrial DNA fragments released during RPE cell death via necrosis or apoptosis. Damage to RPE cells and photoreceptors characterizes advanced dry AMD, notably in geographic atrophy [39] and may lead to the release of cellular debris containing endogenous TLR ligands. TGF-β1 may confer anti-inflammatory effects by suppressing TLR9

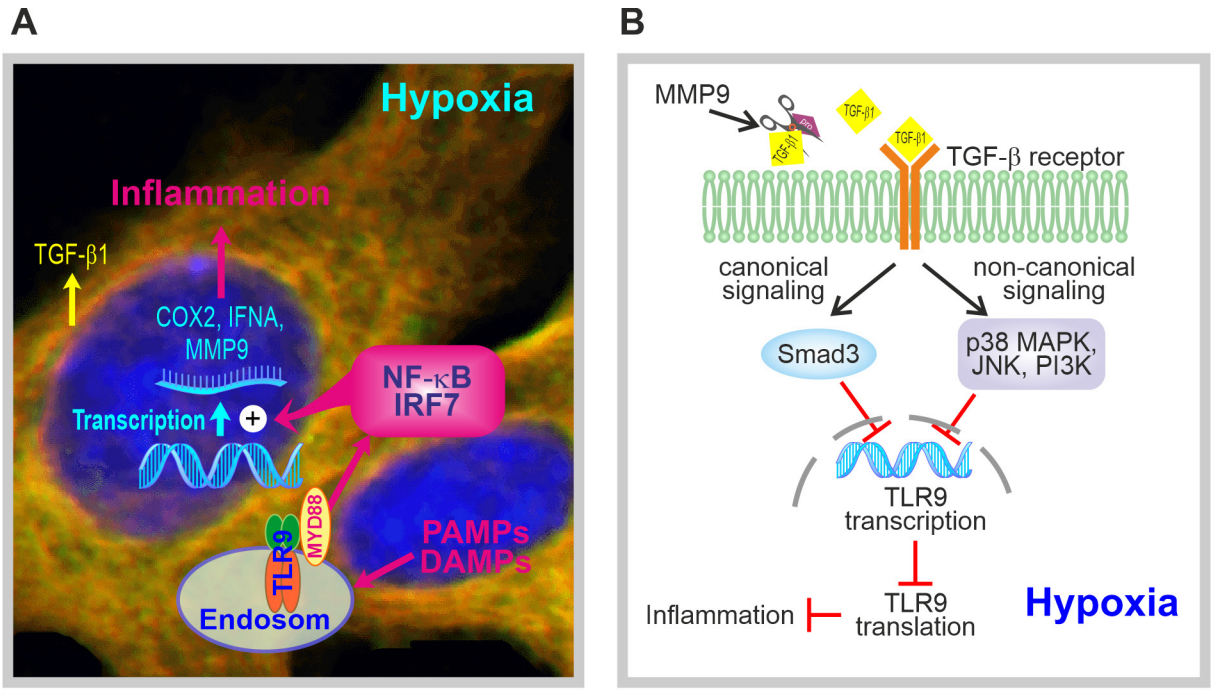

Figure 10. Schematic summary of TLR9 function and TGF-β1 mediated TLR9 expression in cultured human RPE cells **A**: TLR9 effects on gene expression under hypoxia. PAMPs or DAMPs activated TLR9 induces gene expression and activation of *MYD88*, *IRF7*, and NF-κB, leading to upregulation of the gene expression of inflammatory (*COX2, IFNA)* and matrix metalloproteinase *MMP9*. TLR9 seems to play a role in inflammatory processes. Additionally, TLR9 increases the TGF-β1 secretion in cultured RPE cells and thereby TLR9 could inhibit its own gene expression via negative feedback mechanism. **B**: Inhibition of TLR9 by TGF-β1 is mediated by activation via MMP9, binding to the specific receptor and activation of canonical signaling via Smad3 and non-canonical signaling via p38 MAPK, JNK, and PI3K pathways. TGF-β1 seems to mediate an anti-inflammatory effect by inhibiting TLR9. .

expression at both gene and protein levels under normoxic and hypoxic conditions.

APPENDIX 1. SUPPLEMENTAL TABLE 1.

To access the data, click or select the words "Appendix 1." Primer pairs used in qPCR experiments. s, sense. as, antisense. Threshold Cycle (Ct) data are given as mean ± standard deviation (SD) of 7 (TLR1–6) and of 12 (all other genes) independent experiments with RPE cells of different donors cultured under control condition. not detectable - n.d.

APPENDIX 2. SUPPLEMENTAL TABLE 2.

To access the data, click or select the words "Appendix 2." Antibodies used in immunocytochemistry (ICC) and western blot (WB) analysis.

APPENDIX 3. SUPPLEMENTAL FIGURE 1.

To access the data, click or select the words "Appendix 3." *TLR9* gene transcription and mRNA stability. Hyperosmotic and $CoCl_2$-induced expression of the *TLR9* gene is mediated by stimulation of gene transcription in cultured RPE cells. The relative mRNA levels were determined by qPCR and are indicated as fold of control (**A, C**) and as percent of the 0 h control (**B, D**), respectively. **(A)** Chemical hypoxia (150 µM $CoCl_2$, n=4) as well as **(C)** high extracellular osmolarity (+100 mM NaCl, n=4–5) induced *TLR9* gene expression was inhibited by actinomycin D (ActD; 5 µg/ml) that blocks RNA polymerase II. RPE cells were pre-incubated with ActD for 30 min and then for further 6 h with and without NaCl or 24 h with and without $CoCl_2$ respectively. **(B)** *TLR9* stability was not changed under $CoCl_2$-induced hypoxia or **(D)** high extracellular osmolarity compared to untreated controls in cultured RPE cells. The cells were pre-stimulated for 24 h with $CoCl_2$ (n=4), and for 12 h with NaCl (n=3–5) respectively. Then, ActD was added, and RNA was isolated at different time points. (**B Inset**) Ethanol as vehicle of ActD solution had no effect on *TLR9* gene expression (n=4–5). Each bar shows data obtained in independent experiments with cells from different donors. *ACTB* and *B2M* were used to normalize the results obtained with $CoCl_2$ and *ACTB* was used to normalize the NaCl results. Mann–Whitney-U-Test was used for statistical analysis. Significant difference versus unstimulated control: *p<0.05 and to NaCl or $CoCl_2$-control, respectively ● p<0.05 (A, C). Significant difference versus 0 h control: ○ p<0.05 (B, D).

APPENDIX 4. SUPPLEMENTAL FIGURE 2.

To access the data, click or select the words "Appendix 4." Regulation of *MYD88* gene expression in human RPE cells cultured in a 0.1% O_2 atmosphere. Relative mRNA levels were evaluated by qPCR and are shown as folds of unstimulated control. The cells were stimulated for 2, 6, and 24 h, as indicated by the color of the bars. *ACTB* and *B2M* were used to normalize the results. Each bar shows data obtained from 3 to 4 independent experiments with cells from different donors. Statistical analysis was performed using Mann–Whitney-U-Test. Significant difference versus unstimulated control: *p<0.05

APPENDIX 5. SUPPLEMENTAL FIGURE 3.

To access the data, click or select the words "Appendix 5." Effects of inhibitory oligonucleotides for TLR9 on the hyperosmotic gene expression in cultured human RPE cells. The cells were stimulated for 6 h with NaCl (+100 mM), and for 24 h with $CoCl_2$ (150 µM) or in a 0.1% O_2 atmosphere as indicated by the panels of the bars. TLR9 was blocked by iODN 2088 (1 µM) or iODN INH-18 (2.5 µM). As negative control, co-ODN 2088 (co-ODN; 1 and 2.5 µM) was used. The gene expression of **A**. *TLR9* **B.** transcription factor *RELA* (the gene of p65 subunit of transcription factor NF-κB) **C.** *VEGFA,* and **D.** *TGFB1* are presented. The data are shown as fold change of unstimulated control (1). *ACTB* was used to normalize the NaCl results and *ACTB* and *B2M* were used to normalize the PCR results obtained with $CoCl_2$ as well as 0.1% O_2. Mann–Whitney-U-Test was used for statistical analysis. Each bar represents data obtained in 3–6 (iODN 2088) or 3–4 (iODN INH-18) independent experiments using cells from different donors. Significant difference versus unstimulated control: *p<0.05

ACKNOWLEDGMENTS

The authors thank Ute Weinbrecht for excellent technical assistance. All authors have read and agreed to all the content in the manuscript, including the data as presented. The results have not yet been published and are not being considered for publication elsewhere. The data presented in this study are available on request from the corresponding author. FZ has received research grants from DFG, Acylerin, Bayer, Clearside, Kodiak, Johnson&Johnson, Novartis, Ophtea, Regeneron, Roche, Sandoz, speaker honoraria from Allergan/Abbvie, Bayer Healthcare, CME Health, Novartis, Roche and Sanofi and consulting fees from Allergan/Abbvie, Apellis, Alimera, Bayer Healthcare, Biogen, Boehringer-Ingelheim, Roche/Genentech, Johnson&Johnson, NovoNordisk, MSD and Sandoz. All other authors do not have potential conflicts

of interest. Author's contributions: Conceptualization: MH, Formal analysis: EE MH, Funding acquisition: FZ, Investigation: EE HK MH, Methodology: HK MH Project administration: FZ MH, Resources: FZ, Supervision: HK MH, Validation: HK MH, Visualization: EE HK MH, Writing – original draft: EE MH, Writing – review & editing: HK FZ. Funding: This research did not receive any specific grant from funding agencies in the public, commercial, or not-for-profit sectors.

REFERENCES

1. Xu H, Chen M, Forrester JV. Para-inflammation in the aging retina. Prog Retin Eye Res 2009; 28:348-68. [PMID: 19560552].
2. Nita M, Grzybowski A, Ascaso FJ, Huerva V. Age-related macular degeneration in the aspect of chronic low-grade inflammation (pathophysiological parainflammation). Mediators Inflamm 2014; 2014:930671[PMID: 25214719].
3. Kauppinen A, Paterno JJ, Blasiak J, Salminen A, Kaarniranta K. Inflammation and its role in age-related macular degeneration. Cell Mol Life Sci 2016; 73:1765-86. [PMID: 26852158].
4. Johnson LV, Leitner WP, Staples MK, Anderson DH. Complement activation and inflammatory processes in Drusen formation and age related macular degeneration. Exp Eye Res 2001; 73:887-96. [PMID: 11846519].
5. Anderson DH, Mullins RF, Hageman GS, Johnson LV. A role for local inflammation in the formation of drusen in the aging eye. Am J Ophthalmol 2002; 134:411-31. [PMID: 12208254].
6. Anderson DH, Radeke MJ, Gallo NB, Chapin EA, Johnson PT, Curletti CR, Hancox LS, Hu J, Ebright JN, Malek G, Hauser MA, Rickman CB, Bok D, Hageman GS, Johnson LV. The pivotal role of the complement system in aging and age-related macular degeneration: hypothesis re-visited. Prog Retin Eye Res 2010; 29:95-112. [PMID: 19961953].
7. Stanton CM, Wright AF. Inflammatory biomarkers for AMD. Adv Exp Med Biol 2014; 801:251-7. [PMID: 24664705].
8. Ambati J, Ambati BK, Yoo SH, Ianchulev S, Adamis AP. Age-related macular degeneration: etiology, pathogenesis, and therapeutic strategies. Surv Ophthalmol 2003; 48:257-93. [PMID: 12745003].
9. Ishida O, Oku H, Ikeda T, Nishimura M, Kawagoe K, Nakamura K. Is *Chlamydia pneumoniae* infection a risk factor for age related macular degeneration? Br J Ophthalmol 2003; 87:523-4. [PMID: 12714382].
10. Miller DM, Espinosa-Heidmann DG, Legra J, Dubovy SR, Sũner IJ, Sedmak DD, Dix RD, Cousins SW. The association of prior cytomegalovirus infection with neovascular age-related macular degeneration. Am J Ophthalmol 2004; 138:323-8. [PMID: 15364212].
11. Kalayoglu MV, Bula D, Arroyo J, Gragoudas ES, D'Amico D, Miller JW. Identification of *Chlamydia pneumoniae* within human choroidal neovascular membranes secondary to age-related macular degeneration. Graefes Arch Clin Exp Ophthalmol 2005; 243:1080-90. [PMID: 15909160].
12. Robman L, Mahdi O, McCarty C, Dimitrov P, Tikellis G, McNeil J, Byrne G, Taylor H, Guymer R. Exposure to *Chlamydia pneumoniae* infection and progression of age-related macular degeneration. Am J Epidemiol 2005; 161:1013-9. [PMID: 15901621].
13. Kaneko H, Dridi S, Tarallo V, Gelfand BD, Fowler BJ, Cho WG, Kleinman ME, Ponicsan SL, Hauswirth WW, Chiodo VA, Karikó K, Yoo JW, Lee DK, Hadziahmetovic M, Song Y, Misra S, Chaudhuri G, Buaas FW, Braun RE, Hinton DR, Zhang Q, Grossniklaus HE, Provis JM, Madigan MC, Milam AH, Justice NL, Albuquerque RJ, Blandford AD, Bogdanovich S, Hirano Y, Witta J, Fuchs E, Littman DR, Ambati BK, Rudin CM, Chong MM, Provost P, Kugel JF, Goodrich JA, Dunaief JL, Baffi JZ, Ambati J. DICER1 deficit induces Alu RNA toxicity in age-related macular degeneration. Nature 2011; 471:325-30. [PMID: 21297615].
14. Murakami Y, Matsumoto H, Roh M, Giani A, Kataoka K, Morizane Y, Kayama M, Thanos A, Nakatake S, Notomi S, Hisatomi T, Ikeda Y, Ishibashi T, Connor KM, Miller JW, Vavvas DG. Programmed necrosis, not apoptosis, is a key mediator of cell loss and DAMP-mediated inflammation in dsRNA-induced retinal degeneration. Cell Death Differ 2014; 21:270-7. [PMID: 23954861].
15. Takeda K, Kaisho T, Akira S. Toll-like receptors. Annu Rev Immunol 2003; 21:335-76. [PMID: 12524386].
16. Akira S, Uematsu S, Takeuchi O. Pathogen recognition and innate immunity. Cell 2006; 124:783-801. [PMID: 16497588].
17. Trinchieri G, Sher A. Cooperation of Toll-like receptor signals in innate immune defence. Nat Rev Immunol 2007; 7:179-90. [PMID: 17318230].
18. Hemmi H, Takeuchi O, Kawai T, Kaisho T, Sato S, Sanjo H, Matsumoto M, Hoshino K, Wagner H, Takeda K, Akira S. A Toll-like receptor recognizes bacterial DNA. Nature 2000; 408:740-5. [PMID: 11130078].
19. Krieg AM. CpG motifs in bacterial DNA and their immune effects. Annu Rev Immunol 2002; 20:709-60. [PMID: 11861616].
20. Grazioli S, Pugin J. Mitochondrial damage-associated molecular patterns: from inflammatory signaling to human diseases. Front Immunol 2018; 9:832-[PMID: 29780380].
21. Latz E, Schoenemeyer A, Visintin A, Fitzgerald KA, Monks BG, Knetter CF, Lien E, Nilsen NJ, Espevik T, Golenbock DT. TLR9 signals after translocating from the ER to CpG DNA in the lysosome. Nat Immunol 2004; 5:190-8. [PMID: 14716310].
22. Kawasaki T, Kawai T. Toll-like receptor signaling pathways. Front Immunol 2014; 5:461-[PMID: 25309543].
23. Nishimoto S, Fukuda D, Sata M. Emerging roles of Toll-like receptor 9 in cardiometabolic disorders. Inflamm Regen 2020; 40:18-[PMID: 32714475].

24. Kumar MV, Nagineni CN, Chin MS, Hooks JJ, Detrick B. Innate immunity in the retina: Toll-like receptor (TLR) signaling in human retinal pigment epithelial cells. J Neuroimmunol 2004; 153:7-15. [PMID: 15265658].

25. Ebihara N, Chen L, Tokura T, Ushio H, Iwatsu M, Murakami A. Distinct functions between toll-like receptors 3 and 9 in retinal pigment epithelial cells. Ophthalmic Res 2007; 39:155-63. [PMID: 17534115].

26. Fujimoto T, Sonoda KH, Hijioka K, Sato K, Takeda A, Hasegawa E, Oshima Y, Ishibashi T. Choroidal neovascularization enhanced by *Chlamydia pneumoniae* via Toll-like receptor 2 in the retinal pigment epithelium. Invest Ophthalmol Vis Sci 2010; 51:4694-702. [PMID: 20393111].

27. Brosig A, Kuhrt H, Wiedemann P, Kohen L, Bringmann A, Hollborn M. Gene expression regulation in retinal pigment epithelial cells induced by viral RNA and viral/bacterial DNA. Mol Vis 2015; 21:1000-16. [PMID: 26330750].

28. Klettner A, Roider J. Retinal Pigment Epithelium Expressed Toll-like Receptors and Their Potential Role in Age-Related Macular Degeneration. Int J Mol Sci 2021; 22:8387-[PMID: 34445096].

29. Lutty GA, Merges C, Threlkeld AB, Crone S, McLeod DS. Heterogeneity in localization of isoforms of TGF-beta in human retina, vitreous, and choroid. Invest Ophthalmol Vis Sci 1993; 34:477-87. [PMID: 7680639].

30. Kvanta A. Expression and secretion of transforming growth factor-beta in transformed and nontransformed retinal pigment epithelial cells. Ophthalmic Res 1994; 26:361-7. [PMID: 7715917].

31. Yu Q, Stamenkovic I. Cell surface-localized matrix metalloproteinase-9 proteolytically activates TGF-beta and promotes tumor invasion and angiogenesis. Genes Dev 2000; 14:163-76. [PMID: 10652271].

32. Hachana S, Larrivée B. TGF-β Superfamily Signaling in the Eye: Implications for Ocular Pathologies. Cells 2022; 11:2336-[PMID: 35954181].

33. Tosi GM, Orlandini M, Galvagni F. The Controversial Role of TGF-β in Neovascular Age-Related Macular Degeneration Pathogenesis. Int J Mol Sci 2018; 19:3363-[PMID: 30373226].

34. Nagineni CN, Samuel W, Nagineni S, Pardhasaradhi K, Wiggert B, Detrick B, Hooks JJ. Transforming growth factor-beta induces expression of vascular endothelial growth factor in human retinal pigment epithelial cells: involvement of mitogen-activated protein kinases. J Cell Physiol 2003; 197:453-62. [PMID: 14566975].

35. Tosi GM, Caldi E, Neri G, Nuti E, Marigliani D, Baiocchi S, Traversi C, Cevenini G, Tarantello A, Fusco F, Nardi F, Orlandini M, Galvagni F. HTRA1 and TGF-β1 Concentrations in the Aqueous Humor of Patients With Neovascular Age-Related Macular Degeneration. Invest Ophthalmol Vis Sci 2017; 58:162-7. [PMID: 28114575].

36. Dagher Z, Gerhardinger C, Vaz J, Goodridge M, Tecilazich F, Lorenzi M. The Increased Transforming Growth Factor-β Signaling Induced by Diabetes Protects Retinal Vessels. Am J Pathol 2017; 187:627-38. [PMID: 28162229].

37. Naiki Y, Michelsen KS, Zhang W, Chen S, Doherty TM, Arditi M. Transforming growth factor-beta differentially inhibits MyD88-dependent, but not TRAM- and TRIF-dependent, lipopolysaccharide-induced TLR4 signaling. J Biol Chem 2005; 280:5491-5. [PMID: 15623538].

38. Nishimoto S, Sata M, Fukuda D. Expanding role of deoxyribonucleic acid-sensing mechanism in the development of lifestyle-related diseases. Front Cardiovasc Med 2022; 9:881181[PMID: 36176986].

39. Gehrs KM, Anderson DH, Johnson LV, Hageman GS. Age-related macular degeneration–emerging pathogenetic and therapeutic concepts. Ann Med 2006; 38:450-71. [PMID: 17101537].

40. van Leeuwen R, Ikram MK, Vingerling JR, Witteman JC, Hofman A, de Jong PT. Blood pressure, atherosclerosis, and the incidence of age-related maculopathy: the Rotterdam Study. Invest Ophthalmol Vis Sci 2003; 44:3771-7. [PMID: 12939290].

41. Kamoi K, Takeda K, Hashimoto K, Tanaka R, Okuyama S. Identifying risk factors for clinically significant diabetic macula edema in patients with type 2 diabetes mellitus. Curr Diabetes Rev 2013; 9:209-17. [PMID: 23363297].

42. Prager P, Hollborn M, Steffen A, Wiedemann P, Kohen L, Bringmann A. $P2Y_1$ receptor signaling contributes to high salt-induced priming of the NLRP3 inflammasome in retinal pigment epithelial cells. PLoS One 2016; 11:e0165653[PMID: 27788256].

43. Veltmann M, Hollborn M, Reichenbach A, Wiedemann P, Kohen L, Bringmann A. Osmotic induction of angiogenic growth factor expression in human retinal pigment epithelial cells. PLoS One 2016; 11:e0147312[PMID: 26800359].

44. Muñoz-Sánchez J, Chánez-Cárdenas ME. The use of cobalt chloride as a chemical hypoxia model. J Appl Toxicol 2019; 39:556-70. [PMID: 30484873].

45. Pfaffl MW, Tichopad A, Prgomet C, Neuvians TP. Determination of stable housekeeping genes, differentially regulated target genes and sample integrity: BestKeeper–Excel-based tool using pair-wise correlations. Biotechnol Lett 2004; 26:509-15. [PMID: 15127793].

46. Livak KJ, Schmittgen TD. Analysis of relative gene expression data using real-time quantitative PCR and the $2^{(-\Delta\Delta C(T))}$ Method. Methods 2001; 25:402-8. [PMID: 11846609].

47. Campochiaro PA, Wykoff CC, Brown DM, Boyer DS, Barakat M, Taraborelli D, Noronha G. Tanzanite Study Group. Suprachoroidal Triamcinolone Acetonide for Retinal Vein Occlusion: Results of the Tanzanite Study. Ophthalmol Retina 2018; 2:320-8. [PMID: 31047241].

48. Lawless C, Wang C, Jurk D, Merz A, Zglinicki Tv, Passos JF. Quantitative assessment of markers for cell senescence. Exp Gerontol 2010; 45:772-8. [PMID: 20117203].

49. Doyle SE, O'Connell RM, Miranda GA, Vaidya SA, Chow EK, Liu PT, Suzuki S, Suzuki N, Modlin RL, Yeh WC, Lane

TF, Cheng G. Toll-like receptors induce a phagocytic gene program through p38. J Exp Med 2004; 199:81-90. [PMID: 14699082].

50. Blasius AL, Beutler B. Intracellular toll-like receptors. Immunity 2010; 32:305-15. [PMID: 20346772].

51. Khaliq A, Patel B, Jarvis-Evans J, Moriarty P, McLeod D, Boulton M. Oxygen modulates production of bFGF and TGF-beta by retinal cells in vitro. Exp Eye Res 1995; 60:415-23. [PMID: 7789421].

52. Zareparsi S, Buraczynska M, Branham KEH, Shah S, Eng D, Li M, Pawar H, Yashar BM, Moroi SE, Lichter PR, Petty HR, Richards JE, Abecasis GR, Elner VM, Swaroop A. Toll-like receptor 4 variant D299G is associated with susceptibility to age-related macular degeneration. Hum Mol Genet 2005; 14:1449-55. [PMID: 15829498].

53. Dvoriantchikova G, Barakat DJ, Hernandez E, Shestopalov VI, Ivanov D. Toll-like receptor 4 contributes to retinal ischemia/reperfusion injury. Mol Vis 2010; 16:1907-12. [PMID: 21031135].

54. Xu WQ, Wang YS. The role of Toll-like receptors in retinal ischemic diseases. Int J Ophthalmol 2016; 9:1343-51. [PMID: 27672603].

55. Miller JW, Le Couter J, Strauss EC, Ferrara N. Vascular endothelial growth factor a in intraocular vascular disease. Ophthalmology 2013; 120:106-14. [PMID: 23031671].

56. Aceves-Franco LA, Sanchez-Aguilar OE, Barragan-Arias AR, Ponce-Gallegos MA, Navarro-Partida J, Santos A. The Evolution of Triamcinolone Acetonide Therapeutic Use in Retinal Diseases: From Off-Label Intravitreal Injection to Advanced Nano-Drug Delivery Systems. Biomedicines 2023; 11:1901-[PMID: 37509540].

57. Otsuka H, Kawano H, Sonoda S, Nakamura M, Sakamoto T. Particle-induced endophthalmitis: possible mechanisms of sterile endophthalmitis after intravitreal triamcinolone. Invest Ophthalmol Vis Sci 2013; 54:1758-66. [PMID: 23404123].

58. Roth DB, Flynn HW Jr. Distinguishing between infectious and noninfectious endophthalmitis after intravitreal triamcinolone injection. Am J Ophthalmol 2008; 146:346-7. [PMID: 18724979].

59. Kumar V. The Trinity of cGAS, TLR9, and ALRs Guardians of the Cellular Galaxy Against Host-Derived Self-DNA. Front Immunol 2021; 11:624597[PMID: 33643304].

60. Kezic JM, McMenamin PG. Systemic exposure to CpG-ODN elicits low-grade inflammation in the retina. Exp Eye Res 2019; 186:107708[PMID: 31242444].

61. Cheng Z, Yao W, Zheng J, Ding W, Wang Y, Zhang T, Zhu L, Zhou F. A derivative of betulinic acid protects human Retinal Pigment Epithelial (RPE) cells from cobalt chloride-induced acute hypoxic stress. Exp Eye Res 2019; 180:92-101. [PMID: 30578788].

62. Fukuda D, Nishimoto S, Aini K, Tanaka A, Nishiguchi T, Kim-Kaneyama J-R, Lei X-F, Masuda K, Naruto T, Tanaka K, Higashikuni Y, Hirata Y, Yagi S, Kusunose K, Yamada H, Soeki T, Imoto I, Akasaka T, Shimabukuro M, Sata M. Toll-like receptor 9 plays a pivotal role in angiotensin II-induced atherosclerosis. J Am Heart Assoc 2019; 8:e010860[PMID: 30905257].

63. Lim E-J, Lee S-H, Lee J-G, Kim J-R, Yun S-S, Baek S-H, Lee C. Toll-like receptor 9 dependent activation of MAPK and NF-kB is required for the CpG ODN-induced matrix metalloproteinase-9 expression. Exp Mol Med 2007; 39:239-45. [PMID: 17464186].

64. Kawai T, Akira S. TLR signaling. Cell Death Differ 2006; 13:816-25. [PMID: 16410796].

65. Hooks JJ, Nagineni CN, Hooper LC, Hayashi K, Detrick B. IFN-β provides immuno-protection in the retina by inhibiting ICAM-1 and CXCL9 in retinal pigment epithelial cells. J Immunol 2008; 180:3789-96. [PMID: 18322185].

66. Carmeliet P. Angiogenesis in health and disease. Nat Med 2003; 9:653-60. [PMID: 12778163].

67. Kulkarni AB, Huh CG, Becker D, Geiser A, Lyght M, Flanders KC, Roberts AB, Sporn MB, Ward JM, Karlsson S. Transforming growth factor β 1 null mutation in mice causes excessive inflammatory response and early death. Proc Natl Acad Sci U S A 1993; 90:770-4. [PMID: 8421714].

68. Merrell MA, Ilvesaro JM, Lehtonen N, Sorsa T, Gehrs B, Rosenthal E, Chen D, Shackley B, Harris KW, Selander KS. Toll-like receptor 9 agonists promote cellular invasion by increasing matrix metalloproteinase activity. Mol Cancer Res 2006; 4:437-47. [PMID: 16849519].

69. Naik P, Singh S, Vishwakarma S, Kaur I, Dave VP, Kumar A, Joseph J. Multidrug-Resistant *Pseudomonas aeruginosa* Evokes Differential Inflammatory Responses in Human Microglial and Retinal Pigment Epithelial Cells. Microorganisms 2020; 8:735-[PMID: 32423093].

70. Schlecht A, Leimbeck SV, Jägle H, Feuchtinger A, Tamm ER, Braunger BM. Deletion of Endothelial Transforming Growth Factor-β Signaling Leads to Choroidal Neovascularization. Am J Pathol 2017; 187:2570-89. [PMID: 28823871].

71. Naiki Y, Komatsu T, Koide N, Dagvadorj J, Yoshida T, Arditi M, Yokochi T. TGF-β1 inhibits the production of IFN in response to CpG DNA via ubiquitination of TNF receptor-associated factor (TRAF) 6. Innate Immun 2015; 21:770-7. [PMID: 26224488].

72. Kaur B, Miglioranza Scavuzzi B, F Abcouwer S, N Zacks D. A simplified protocol to induce hypoxia in a standard incubator: A focus on retinal cells. Exp Eye Res 2023; 236:109653[PMID: 37793495].